

Chempath 1.0: An open-source pathway analysis program for photochemical models

Daniel Garduno Ruiz¹, Colin Goldblatt¹, and Anne-Sofie Ahm¹

¹School of Earth and Ocean Sciences, University of Victoria, Victoria, British Columbia, Canada

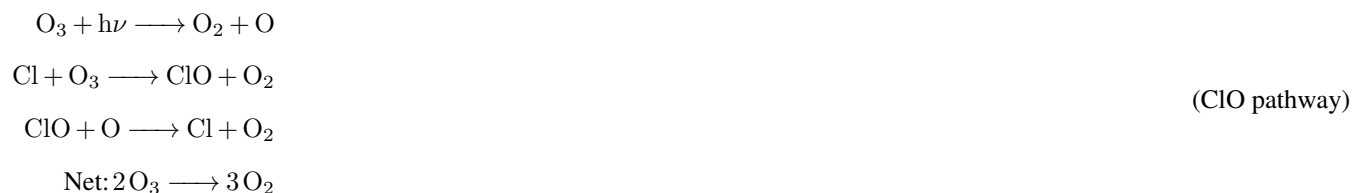
Correspondence: Daniel Garduno Ruiz (danielgardunoruiz@uvic.ca)

Abstract. We describe the development of *Chempath*: an open-source pathway analysis program for photochemical models. This algorithm can help understand the results of complex photochemical models by identifying the most important reaction chains (pathways) for the production and destruction of a species of interest in a reaction system. The algorithm can also quantify the contribution of the pathways to the production and destruction of a species. *Chempath* is a Python re-implementation of the algorithm developed by Lehmann (2004).

We demonstrate how to apply *Chempath* to a one-dimensional photochemical model, using an example of a reaction system for Earth’s present-day atmosphere. *Chempath* can identify well-known chemical mechanisms for O₃ production and destruction in this model, suggesting that this algorithm can be applied to understand photochemical models of less well-known atmospheres, like past and exoplanet atmospheres.

1 Introduction

The construction of chemical pathways is essential to understand the results of photochemical models. These models typically represent hundreds of reactions producing and destroying chemical species within the atmosphere (see for example Hu et al. 2012; Tsai et al. 2017; Wogan et al. 2022). The interaction of these reactions makes it difficult to attribute the production or destruction of a species to a single reaction. Instead, to understand the mechanisms that affect the concentration of a species it is necessary to construct pathways. A pathway is a sequence of reactions that interact with each other to produce, destroy, or recycle a species. For example, stratospheric ozone destruction is explained in terms of pathways that catalyze O₃ destruction (Lary, 1997). One of these pathways involves the reaction of O₃ with chlorine species (Molina and Rowland, 1974):



This ozone-destructing pathway has three reactions, and its net effect is to convert two O₃ molecules into three O₂ molecules.

20 Several methods can help understand the results of photochemical models. For example, sensitivity analyses can constrain uncertainties in reaction rate constants and provide information on how variable the results of a model are when the reaction rates are perturbed (Turányi and Tomlin, 2014). Wiring diagrams can help understand the flow of molecules in a reaction system (Fishtik et al., 2006; Androulakis, 2006). However, these methods can not give quantitative information about the chains of reactions responsible for the production or destruction of a species in a chemical model. To understand these chemical mechanisms, it is necessary to construct pathways.

Chemical pathways are usually constructed manually and empirically, tracking and connecting reactions important for the production or destruction of a species of interest. This approach is the most widely used for pathway construction. However, the manual construction of pathways can not give a quantitative estimate of how important a pathway is for the production or destruction of a species relative to other pathways. Also, the manual construction of pathways has reproducibility limitations. 30 Alternatively, pathways can be automatically constructed using algorithms (Milner, 1964; Schuster and Schuster, 1993; Clarke, 1988; Lehmann, 2002, 2004).

One of the most used algorithms to construct pathways is the "Pathway analysis program" created by Lehmann (2004). This algorithm can automatically construct all the significant pathways in a reaction system and calculate the contribution of each pathway to the production and destruction of a species of interest. The "Pathway analysis program" has been used in several studies to gain a better understanding of atmospheric chemistry models (Grenfell et al., 2006; Verronen et al., 2011; Stock et al., 2012a, b; Verronen and Lehmann, 2013; Stock et al., 2017; Gebauer et al., 2017). 35

In this paper, we describe the development of *Chempath*: an open-source Python re-implementation of Lehmann's (2004) algorithm for analysis of photochemical models. We aim to contribute this open-source pathway analysis program to enhance the applicability of this algorithm to photochemical models and to enhance the replicability of chemical pathway construction. We demonstrate how to apply this algorithm to the one-dimensional photochemical model *photochem* (Wogan et al. 2023, <https://github.com/Nicholaswogan/photochem>). *Photochem* is an updated version of *Photochempy* (Wogan, 2023), a model that has been used for exoplanet and early Earth photochemical studies (Wogan et al., 2022; Thompson et al., 2022; Garduno Ruiz et al., 2023, 2024). This model originates from *Atmos*, a photochemical model extensively used to investigate photochemistry in exoplanet and past atmospheres (see for example Kasting et al. 1979; Kasting and Donahue 1980; Segura et al. 2005; Zahnle et al. 2006; Claire et al. 2014; Arney et al. 2016). 45

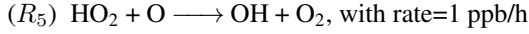
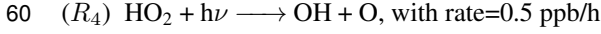
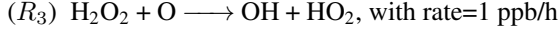
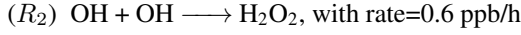
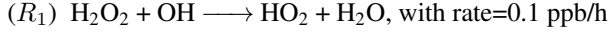
The structure of the paper is as follows. In section 2, we review the Lehmann (2004) algorithm via a simple example. In section 3, we describe how we implemented *Chempath*. In section 4, we demonstrate how to apply *Chempath* to the one-dimensional photochemical model *photochem*.

2 Algorithm review

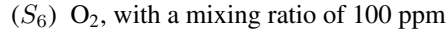
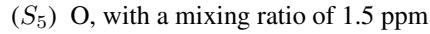
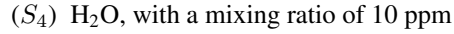
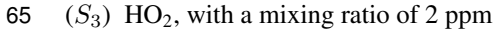
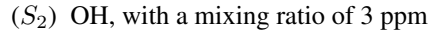
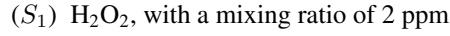
50 Here we provide a summary of the pathway analysis program presented in Lehmann (2004), using a simple example to explain each step of the algorithm (see the original paper for further details). The pathway analysis program forms pathways by the iterative connection of reactions through branching-point species (figure 1). A branching-point species is one that is used to

connect reactions that produce the species with reactions that destroy it. For example, the reaction $\text{Cl} + \text{O}_3 \longrightarrow \text{ClO} + \text{O}_2$ can be connected with the reaction $\text{ClO} + \text{O} \longrightarrow \text{Cl} + \text{O}_2$ through the branching-point species ClO.

55 The example we use to demonstrate the algorithm consists of five reactions between six species involving hydrogen oxide radicals. The reactions are:



and the species are:



We arbitrarily select these rates and mixing ratios for this example. Assuming this reaction system was run for 1 hour, the
70 production and destruction by the reactions result in concentration changes of -0.5, 1.2, -0.4, 0.1, -1.5, and 1 ppb for each species respectively. In the next sections, we will identify which combination of reactions is the most important to explain the OH concentration change.

2.1 Assumptions and definitions

The algorithm uses the variables listed in table 1 to construct pathways. In all the variables $i = 1, \dots, n_s, j = 1, \dots, n_r$ and
75 $k = 1, \dots, n_p$ where n_s is the number of species, n_r is the number of reactions and n_p is the number of pathways. We use two square brackets to denote variables that represent matrices (for example $[[s_{ij}]]$), and one to denote vectors (for example $[c_i]$).

In large reaction systems, it might not be possible to construct all the pathways of the system because the number of pathways could be computationally unmanageable. The algorithm includes the option to delete unimportant pathways to avoid the construction of an unmanageable number of pathways and enhance the computation time. However, the algorithm includes
80 variables to keep track of the rates of these deleted pathways.

Variable	Initial value in simple example	Units in simple example	Description
$[[s_{ij}]]$	$ \begin{array}{ccccc} R_1 & R_2 & R_3 & R_4 & R_5 \\ \begin{pmatrix} -1 & 1 & -1 & 0 & 0 \\ -1 & -2 & 1 & 1 & 1 \\ 1 & 0 & 1 & -1 & -1 \\ 1 & 0 & 0 & 0 & 0 \\ 0 & 0 & -1 & 1 & -1 \\ 0 & 0 & 0 & 0 & 1 \end{pmatrix} & S_1 & S_2 & S_3 & S_4 & S_5 & S_6 \end{array} $	ppb	Stoichiometric matrix representing the number of molecules of species S_i produced ($s_{ij} > 0$) or destroyed ($s_{ij} < 0$) by reaction R_j . For example, in the simple example reaction R_2 destroys two molecules of species S_2 , so $s_{22} = -2$.
dt	1	h	Time step.
$[dc_i]$	$ \begin{array}{ccccc} S_1 & S_2 & S_3 & S_4 & S_5 & S_6 \\ \begin{bmatrix} -0.5 & 1.2 & -0.4 & 0.1 & -1.5 & 1 \end{bmatrix} \end{array} $	ppb	Change in concentration of species S_i in the time step dt .
$[\bar{c}_i]$	$ \begin{array}{ccccc} S_1 & S_2 & S_3 & S_4 & S_5 & S_6 \\ \begin{bmatrix} 1.75 & 3.6 & 1.8 & 10.05 & 0.75 & 100.5 \end{bmatrix} \end{array} $	ppb	Mean concentration of species S_i in the time step dt .
$[\delta_i] = \frac{[dc_i]}{dt}$	$ \begin{array}{ccccc} S_1 & S_2 & S_3 & S_4 & S_5 & S_6 \\ \begin{bmatrix} -0.5 & 1.2 & -0.4 & 0.1 & -1.5 & 1 \end{bmatrix} \end{array} $	ppb/h	Rate of concentration change of species S_i .
$[f_k]$	$ \begin{array}{ccccc} P_1 & P_2 & P_3 & P_4 & P_5 \\ \begin{bmatrix} 0.1 & 0.6 & 1 & 0.5 & 1 \end{bmatrix} \end{array} $	ppb/h	Rate of pathway P_k .
$[r_j]$	$ \begin{array}{ccccc} R_1 & R_2 & R_3 & R_4 & R_5 \\ \begin{bmatrix} 0.1 & 0.6 & 1 & 0.5 & 1 \end{bmatrix} \end{array} $	ppb/h	Mean rate of reaction R_j in time step dt .
$[\tilde{r}_j]$	$ \begin{array}{ccccc} R_1 & R_2 & R_3 & R_4 & R_5 \\ \begin{bmatrix} 0 & 0 & 0 & 0 & 0 \end{bmatrix} \end{array} $	ppb/h	Part of the rate of reaction R_j associated with deleted pathways.

$[\tilde{p}_i]$	$\begin{array}{cccccc} S_1 & S_2 & S_3 & S_4 & S_5 & S_6 \\ \left[\begin{array}{cccccc} 0 & 0 & 0 & 0 & 0 & 0 \end{array} \right] \end{array}$	ppb/h	Rate of production of species S_i by deleted pathways.
$[\tilde{d}_i]$	$\begin{array}{cccccc} S_1 & S_2 & S_3 & S_4 & S_5 & S_6 \\ \left[\begin{array}{cccccc} 0 & 0 & 0 & 0 & 0 & 0 \end{array} \right] \end{array}$	ppb/h	Rate of destruction of species S_i by deleted pathways.
$[p_i] = [\tilde{p}_i] + \sum_{k=1}^{n_p} [[m_{ik}]] \cdot [f_k]$ <p>for $[[m_{ik}]] > 0$</p>	$\begin{array}{cccccc} S_1 & S_2 & S_3 & S_4 & S_5 & S_6 \\ \left[\begin{array}{cccccc} 0.6 & 2.5 & 1.1 & 0.1 & 0.5 & 1 \end{array} \right] \end{array}$	ppb/h	Rate of production of species S_i by all pathways (including deleted pathways).
$[d_i] = [\tilde{d}_i] + \sum_{k=1}^{n_p} [[m_{ik}]] \cdot [f_k]$ <p>for $[[m_{ik}]] < 0$</p>	$\begin{array}{cccccc} S_1 & S_2 & S_3 & S_4 & S_5 & S_6 \\ \left[\begin{array}{cccccc} 1.1 & 1.3 & 1.5 & 0 & 2. & 0 \end{array} \right] \end{array}$	ppb/h	Rate of destruction of species S_i by all pathways (including deleted pathways).
$[[x_{jk}]]$	$\begin{array}{ccccc} P_1 & P_2 & P_3 & P_4 & P_5 \\ \left(\begin{array}{ccccc} 1 & 0 & 0 & 0 & 0 \\ 0 & 1 & 0 & 0 & 0 \\ 0 & 0 & 1 & 0 & 0 \\ 0 & 0 & 0 & 1 & 0 \\ 0 & 0 & 0 & 0 & 1 \end{array} \right) \begin{array}{l} R1 \\ R2 \\ R3 \\ R4 \\ R5 \end{array} \end{array}$	No units	Matrix representing the multiplicity of reaction R_j in pathway P_k . A multiplicity is the number of times a reaction occurs in a pathway. For example, in the ClO pathway presented above all reactions have multiplicities equal to 1. If a reaction does not occur in a pathway, $[[x_{jk}]] = 0$. Initially, this matrix is set equal to an identity matrix with the size of the number of reactions n_r .

$[[m_{ik}]] = \sum_{j=1}^{n_r} [[s_{ij}]] \cdot [[x_{jk}]]$	$\begin{matrix} P_1 & P_2 & P_3 & P_4 & P_5 \\ \begin{pmatrix} -1 & 1 & -1 & 0 & 0 \\ -1 & -2 & 1 & 1 & 1 \\ 1 & 0 & 1 & -1 & -1 \\ 1 & 0 & 0 & 0 & 0 \\ 0 & 0 & -1 & 1 & -1 \\ 0 & 0 & 0 & 0 & 1 \end{pmatrix} & \begin{matrix} S_1 \\ S_2 \\ S_3 \\ S_4 \\ S_5 \\ S_6 \end{matrix} \end{matrix}$	ppb	Matrix representing the number of molecules of species S_i produced ($[[m_{ik}]] > 0$) or destroyed ($[[m_{ik}]] < 0$) by pathway P_k . This variable is equal to the matrix multiplication of $[[s_{ij}]]$ and $[[x_{jk}]]$.
$[\tau_i] = \frac{[c_i^-]}{[d_i]}$	$\begin{matrix} S_1 & S_2 & S_3 & S_4 & S_5 & S_6 \\ \begin{bmatrix} 1.59 & 2.77 & 1.2 & \text{Nan} & 0.38 & \text{Nan} \end{bmatrix} \end{matrix}$	h	Lifetime of species S_i . If the destruction by all pathways $[d_i]$ is zero, the lifetime becomes undefined (Nan). This means that there are no pathways consuming S_i .

Table 1: Variables used in the pathway analysis algorithm and their initial values in the simple example used to explain the algorithm. In all the variables $i = 1, \dots, n_s, j = 1, \dots, n_r$ and $k = 1, \dots, n_p$ where n_s is the number of species, n_r is the number of reactions and n_p is the number of pathways.

The algorithm assumes that the reactions are unidirectional and that the user splits the reversible reactions into their forward and backward components. It is also assumed that mass is conserved in the analyzed chemical model, and the reactions produce the exact number of molecules to explain the concentration changes:

$$[dc_i] = \sum_{j=1}^{n_r} [[s_{ij}]] \cdot [r_j] dt, \quad i = 1 \dots n_s. \quad (1)$$

85 For example, in our simple example we can verify that this condition is satisfied for OH (S_2):

$$dc_2 = \sum_{j=1}^5 [s_{2j}] \cdot [r_j] dt = (-1 \cdot 0.1 - 2 \cdot 0.6 + 1 \cdot 1 + 1 \cdot 0.5 + 1 \cdot 1) \text{ ppb/h} \cdot 1 \text{ h} = 1.2 \text{ ppb} \quad (2)$$

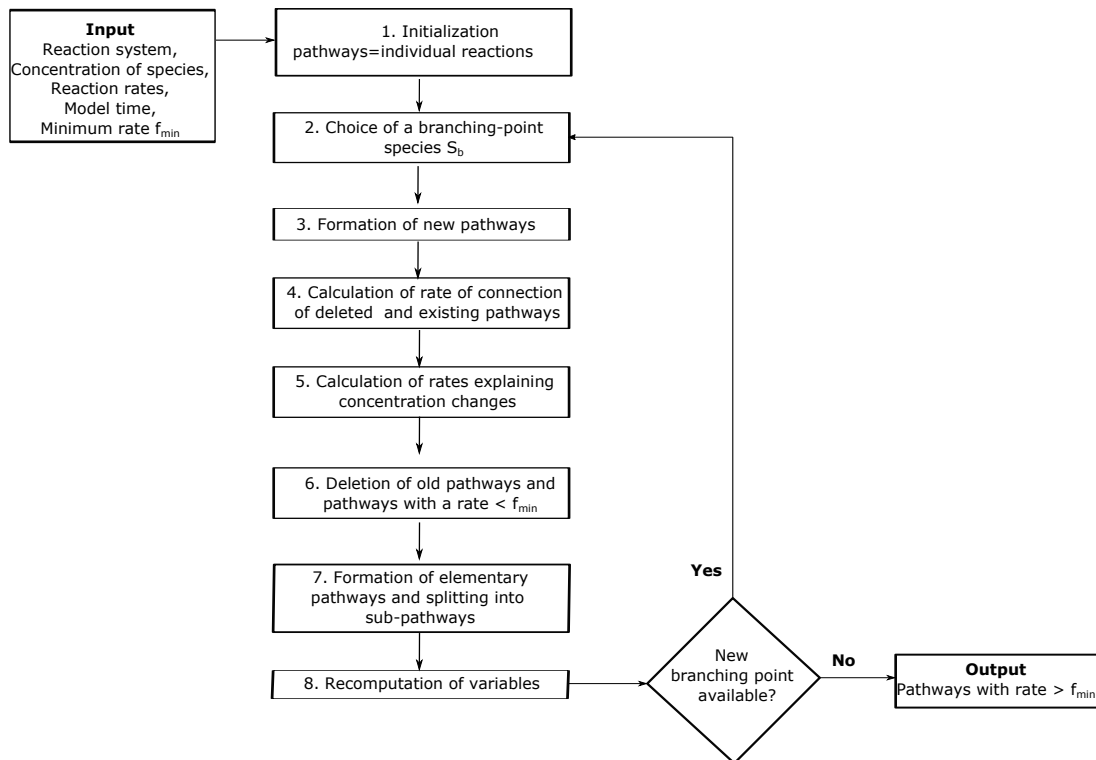


Figure 1. Pathway analysis Program algorithm. For a full description of the algorithm see Lehmann (2004).

2.2 Algorithm initialization

The algorithm requires four inputs from a chemical kinetics model: the species concentrations and the model time in two consecutive model times t and $t + dt$, the mean reaction rates in the time step dt , and the reaction system with n_r reactions between n_s species. The consecutive model time steps must be the time steps in which the solver obtains a solution for the system of equations. The algorithm could also be applied in two model times that are not consecutive, but the time step must be small enough to resolve the processes one is interested in understanding. The user can also input a minimum rate of pathways f_{\min} . With these inputs, the algorithm determines all pathways with a rate $> f_{\min}$. In the simple example, we will use a minimum rate of pathways $f_{\min} = 0.05$ ppb/h.

The algorithm uses the input information to initialize the variables listed in table 1. At first, each pathway is considered to have only one reaction, and the matrix $[[x_{jk}]]$ is initialized as an identity matrix with the size of the number of reactions. This means that initially, pathway P_1 only contains reaction R_1 , pathway P_2 only contains reaction R_2 , etc. The rates of the pathways are initialized with the rates of the reactions: $[f_j] = [r_j]$. The variables $[\tilde{r}_j]$, $[\tilde{p}_i]$, and $[\tilde{d}_i]$ that store rates associated with deleted pathways are initialized as arrays of zeros.

Once the algorithm has been initialized, the next step is to choose a branching point species S_b to start constructing pathways. Species with lower lifetimes are selected as branching-point species first because a small lifetime is associated with fast consumption by reactions. The algorithm forms new pathways through the iterative connection of previously formed pathways through branching-point species until there are no more branching-point species left (figure 1). A species can be a branching-point species only once. To find pathways that destroy or produce a specific species of interest, the species itself is not used as a branching-point. Otherwise, the pathways producing and consuming this species would be connected. Sometimes it is useful to treat some species as inert or long-lived, not considering them as branching-point species. For example, in the atmosphere N_2 is long-lived and inert, so it could not be considered as a branching-point.

In the simple example, where we are investigating the change in OH, we will treat H_2O and O_2 as a long-lived inert species, not considering them as branching-points. The species with the lowest lifetime is O ($\tau_5 = 0.38$ h), so this species is the first branching-point.

2.4 Formation of new pathways and rate calculations

The algorithm forms new pathways connecting all previously formed pathways that produce a branching-point species S_b with all pathways that destroy S_b . The connections are made ensuring that the new pathways do not produce nor destroy the branching-point species S_b . If a pathway P_k produces m_{bk} molecules of the branching-point species S_b and a pathway P_l destroys m_{bl} molecules of S_b , the connection of these pathways forms a new pathway P_n with multiplicities:

$$[x_{jn}] = |m_{bl}|[x_{jk}] + m_{bk}[x_{jl}] \quad (3)$$

where $j = 1 \dots n_r$, k and l are the indexes of the pathways producing and destroying S_b , and b is the index of the species S_b . The rate f_n of the new pathway P_n is calculated by multiplying the rates of the producing (f_k) and destructing (f_l) pathways and dividing by the maximum of the rate of production and destruction of the branching-point species by all pathways:

$$f_n = \frac{f_k f_l}{\max(p_b, d_b)}, \quad (4)$$

where k and l are the indexes of the pathways producing and destroying the branching-point species S_b , and b is the index of the branching-point species. This equation is derived by calculating the rate at which the molecules of S_b formed by P_k are destroyed by P_l (see Lehmann 2004 for the derivation). One can think of equation 4 as distributing the rate of a pathway to new pathways using the probability that a molecule produced (or consumed) by one pathway is consumed (or produced) by another pathway. For example, if the change in concentration of the branching-point species $dc_b > 0$, then the chemical production is greater than the chemical destruction ($p_b > d_b$), and equation 4 takes the form $f_n = \frac{f_k f_l}{p_b}$. The ratio $\pi = \frac{f_k}{p_b}$ can be interpreted as the probability that a molecule of the branching-point species is produced by the pathway P_k . Since the pathway P_l is

going to be connected with all pathways P_k producing S_b , and the sum of the probabilities π over all pathways producing the
 130 branching-point species S_b is equal to one, the rate f_l is going to be completely distributed to the new pathways.

The multiplicities x_{jn} of the new pathway are divided by their greatest common divisor g to keep them as simple as possible. The rate of the new pathway is multiplied by g to avoid altering the number of molecules that the new pathway produces or destroys. The new pathway and its rate are appended to $[[x_{jk}]]$ and $[f_k]$ respectively.

In the simple example, there are two pathways destroying the branching-point species O (P_3 and P_5), and one pathway
 135 producing it (P_4). The connection of these pathways will result in two new pathways. For example, the pathway P_3 destroys one O molecule ($m_{53} = -1$), and the pathway P_4 produces one O molecule ($m_{54} = 1$), so the connection of these pathways results in a new pathway with multiplicities:

$$[x_{jn}] = |m_{53}|[x_{j4}] + m_{54}[x_{j3}] = [0, 0, 0, 1, 0] + [0, 0, 1, 0, 0] = [0, 0, 1, 1, 0]. \quad (5)$$

The rate of this new pathway is:

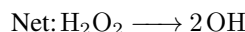
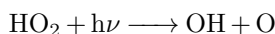
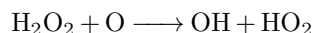
$$140 \quad f_n = \frac{f_4 f_3}{\max(p_5, d_5)} = \frac{0.5 \text{ ppb/h} \cdot 1 \text{ ppb/h}}{2 \text{ ppb/h}} = 0.25 \text{ ppb/h} \quad (6)$$

After forming all new pathways at the branching-point species O, the multiplicities $[[x_{jk}]]$ and the pathway rates $[f_k]$ will have the following form:

$$[[x_{jk}]] = \begin{pmatrix} P_1 & P_2 & P_3 & P_4 & P_5 & P_6 & P_7 \\ 1 & 0 & 0 & 0 & 0 & 0 & 0 \\ 0 & 1 & 0 & 0 & 0 & 0 & 0 \\ 0 & 0 & 1 & 0 & 0 & 1 & 0 \\ 0 & 0 & 0 & 1 & 0 & 1 & 1 \\ 0 & 0 & 0 & 0 & 1 & 0 & 1 \end{pmatrix} \begin{matrix} R_1 \\ R_2 \\ R_3 \\ R_4 \\ R_5 \end{matrix} \quad (7)$$

$$[f_k] = \begin{bmatrix} P_1 & P_2 & P_3 & P_4 & P_5 & P_6 & P_7 \\ 0.1 & 0.6 & 1 & 0.5 & 1 & 0.25 & 0.25 \end{bmatrix} \text{ ppb/h}$$

We can think of a column in $[[x_{jk}]]$ as a pathway. For example, the pathway that we formed before (P_6) is located in the 6th
 145 column of the matrix $[[x_{jk}]]$ in equation 7, and contains one times reaction R_3 and one times reaction R_4 :



(P_6)

2.5 Calculation of rate of connection of deleted and existing pathways

In this step, the algorithm calculates the rates of the connection of deleted pathways with existing pathways. Pathways with a rate lower than f_{\min} will be deleted in a subsequent step (see section 2.7). In the first iteration of the algorithm there are no deleted pathways, but in other iterations some pathways could have been deleted by this point. In that case, the deleted pathways can not be connected with existing pathways. However, the algorithm keeps track of the rates of production and destruction of the branching-point species S_b that would have been computed in these connections. The deleted pathways produce the branching-point species S_b at a rate \tilde{p}_b , so according to equation 4, the rate of the connection of deleted pathways that produce S_b with an existing pathway P_e that destroys S_b is:

$$\tilde{f}_e = \frac{f_e \tilde{p}_b}{\max(p_b, d_b)}, \quad (8)$$

where e represents the index of the pathway that destroys the branching-point species S_b . Similarly, deleted pathways consuming S_b at a rate \tilde{d}_b would have been connected with an existing pathway P_e producing S_b at a rate:

$$\tilde{f}_e = \frac{f_e \tilde{d}_b}{\max(p_b, d_b)}, \quad (9)$$

where e represents the index of the pathway that produces S_b . This rate is added to the the variables $[\tilde{r}_j]$, $[\tilde{p}_i]$ and $[\tilde{d}_i]$ that store rates associated with deleted pathways:

$$\begin{aligned} [\tilde{r}_j] &= [\tilde{r}_j] + [x_{je}] \cdot \tilde{f}_e \\ [\tilde{p}_i] &= [\tilde{p}_i] + [m_{ie}] \cdot \tilde{f}_e \quad \text{for } [m_{ie}] > 0 \\ [\tilde{d}_i] &= [\tilde{d}_i] + |[m_{ie}]| \cdot \tilde{f}_e \quad \text{for } [m_{ie}] < 0 \end{aligned} \quad (10)$$

where $i = 1 \dots n_s, j = 1 \dots n_r, e = \text{index of pathway producing or destroying the branching-point species } S_b$. These operations are repeated for all existing pathways producing and destroying the branching-point species. In the simple example, there are no deleted pathways yet, so $\tilde{f}_e = 0$.

2.6 Calculation of rates explaining concentration changes

In this step, the algorithm redefines the rates of the pathways that contribute to the concentration change of the branching-point species S_b . The pathways that produce molecules of the branching point species S_b contribute to its concentration change dc_b if $dc_b > 0$. Similarly, the pathways that destroy molecules of the branching point species S_b contribute to its concentration change dc_b if $dc_b < 0$. The algorithm redefines the rate f_k of pathways contributing to the concentration change of the branching-point-species, keeping the fraction \hat{f}_k of f_k that contributes to the concentration change dc_b . This fraction is calculated by

multiplying the rate f_k by the absolute value of the rate of concentration change of the branching point species δ_b , and dividing by the maximum of the production and destruction of the branching-point species by all pathways:

$$\hat{f}_k = \frac{f_k |\delta_b|}{\max(p_b, d_b)} \quad (11)$$

where k = index of the pathway producing or destroying S_b , and b is the index of the branching-point species S_b . This rate is derived by calculating the probability that a molecule of S_b produced or destroyed by a pathway contributes to the concentration change of the branching point species dc_b (see Lehmann 2004 for the derivation). If $dc_b = 0$ there is no redefinition of rates.

In the simple example, the branching-point species O has a concentration change $dc_5 = -1.5$ ppb. Since $dc_5 < 0$, we will redefine the rates of the pathways that destroy O because they contribute to the concentration change dc_5 . For example, the pathway P_3 has a single reaction destroying O at a rate of 1 ppb/h. The part of this rate that contributes to the O concentration change is:

$$\hat{f}_3 = \frac{f_3 |\delta_5|}{\max(p_5, d_5)} = \frac{1 \text{ ppb/h} \cdot 1.5 \text{ ppb/h}}{2 \text{ ppb/h}} = 0.75 \text{ ppb/h}. \quad (12)$$

After all the rates of the pathways destroying S_b are redefined, $[f_k]$ has the form:

$$[f_k] = \begin{bmatrix} P_1 & P_2 & P_3 & P_4 & P_5 & P_6 & P_7 \\ 0.1 & 0.6 & 0.75 & 0.5 & 0.75 & 0.25 & 0.25 \end{bmatrix} \text{ ppb/h} \quad (13)$$

2.7 Deletion of old pathways and pathways with a rate $< f_{\min}$

After a pathway producing the branching-point species S_b has been connected with all pathways destroying S_b , it is eliminated from the matrix $[[x_{jk}]]$ if it does not contribute to the concentration change dc_b . If $dc_b > 0$, the pathways that destroy the branching-point species are deleted. If $dc_b < 0$, the pathways that produce the branching-point species are deleted, and if $dc_b = 0$, both the pathways that produce and destroy the branching-point species are deleted.

In the simple example $dc_5 < 0$, so the pathways P_3 and P_5 that were used to form new pathways will not be deleted because they destroy molecules of the branching-point species O, contributing to its concentration change. However, the pathway P_4 does not contribute to dc_5 , so it is deleted.

The algorithm also deletes pathways with a rate $< f_{\min}$ to avoid constructing an unmanageable number of pathways and to enhance the computing time. If there are n_q pathways with rate $f_q < f_{\min}$, these pathways are deleted from the matrix $[[x_{jk}]]$ and the the variables $[\tilde{r}_j]$, $[\tilde{p}_i]$ and $[\tilde{d}_i]$ are updated according to:

$$\begin{aligned}
[\tilde{r}_j] &= [\tilde{r}_j] + \sum_q [x_{jq}] \cdot [f_q] \\
195 \quad [\tilde{p}_i] &= [\tilde{p}_i] + \sum_q [m_{iq}] \cdot [f_q] \quad \text{for } [m_{iq}] > 0 \\
[\tilde{d}_i] &= [\tilde{d}_i] + \sum_q |[m_{iq}]| \cdot [f_q] \quad \text{for } [m_{iq}] < 0
\end{aligned} \tag{14}$$

where $i = 1 \dots n_s, j = 1 \dots n_r$, and $q = \text{indexes of pathways with rate } < f_{\min}$. The rates of these pathways are also deleted from the array $[f_k]$.

In the simple example, none of the pathways have a rate $< f_{\min}$, so there is no deletion of pathways in this first iteration. See section 2.10 to see an example of how pathways with a rate $< f_{\min}$ are deleted. After this step, the multiplicities $[[x_{jk}]]$ and the
200 pathway rates $[f_k]$ will have the following form:

$$[[x_{jk}]] = \begin{pmatrix} P_1 & P_2 & P_3 & P_4 & P_5 & P_6 \\ 1 & 0 & 0 & 0 & 0 & 0 \\ 0 & 1 & 0 & 0 & 0 & 0 \\ 0 & 0 & 1 & 0 & 1 & 0 \\ 0 & 0 & 0 & 0 & 1 & 1 \\ 0 & 0 & 0 & 1 & 0 & 1 \end{pmatrix} \begin{matrix} R_1 \\ R_2 \\ R_3 \\ R_4 \\ R_5 \end{matrix} \tag{15}$$

$$[f_k] = \begin{matrix} P_1 & P_2 & P_3 & P_4 & P_5 & P_6 \\ \begin{bmatrix} 0.1 & 0.6 & 0.75 & 0.75 & 0.25 & 0.25 \end{bmatrix} \end{matrix} \text{ ppb/h}$$

Note that when pathways are deleted from the matrix $[[x_{jk}]]$ there is a redefinition of pathways. For example, since pathway P_4 was deleted, now there is a new pathway P_4 that corresponds to the fourth column of $[[x_{jk}]]$ in equation 15.

2.8 Formation of elementary pathways and splitting into sub-pathways

205 The steps above can produce pathways with a large and unnecessary number of reactions. The algorithm splits these complex pathways into shorter, simpler pathways. The first step in this process is to find the elementary sub-pathways of a complex pathway. A pathway P_s is a sub-pathway of a pathway P_c if all the reactions in P_s are in P_c . Elementary pathways do not have sub-pathways. The algorithm finds the elementary sub-pathways of a pathway P_c by forming new pathways with the reactions contained in P_c and keeping only the elementary pathways (see Lehmann 2004 for a full description of this process). If a
210 pathway P_c with multiplicities $[x_{jc}]$ has n_e elementary sub-pathways with multiplicities $[[x'_{je}]]$, the algorithm splits $[x_{jc}]$ into the sub-pathways $[[x'_{je}]]$ finding weighs $[w_e]$ that fulfill the equation:

$$[x_{jc}] = \sum_{e=1}^{n_e} [w_e] \cdot [[x'_{je}]], \text{ where } j = 1 \dots n_r \text{ and } c = \text{index of pathway to be split.} \quad (16)$$

The rate f_c of the pathway P_c is distributed to the sub-pathways using the weights $[w_e]$:

$$[f_e] = f_c [w_e], \text{ where } e = 1 \dots n_e, \text{ and } c = \text{index of pathway to be split.} \quad (17)$$

215 After finding the sub-pathways, the algorithm deletes $[x_{jc}]$ from $[[x_{jk}]]$ and appends the new-sub pathways $[[x'_{je}]]$ into $[[x_{jk}]]$. Similarly, the rate f_c is deleted, and the rates $[f_e]$ are appended to $[f_k]$. If a sub-pathway already exists in the matrix $[[x_{jk}]]$, its rate is added to the already existing pathway.

As noted by Lehmann (2004), equation 16 can have multiple solutions, leading to slightly different results according to the solution that one chooses. However, these differences tend to be small and the overall result of the algorithm is similar even
 220 when equation 16 has multiple solutions (Lehmann, 2004). Our implementation includes two options to solve equation 16. The first option uses Scipy's "lsq_linear" function, minimizing the expression:

$$0.5 ||Ax - b||^2 \text{ with constraints } 0 \leq x < \infty, \quad (18)$$

where $||x||$ is the norm of x , $A = [[x'_{je}]]$, $x = [w_e]$ and $b = [x_{jc}]$. When there are multiple solutions to equation 16, we choose the first solution that minimizes equation 18 found by the "lsq_linear" algorithm. The second option to solve equation
 225 16 implements the method proposed in section 5.2.2 of (Lehmann, 2004). This method chooses the solution that produces more probable pathways in the sense that this solution produces simpler pathways with higher rates compared to other solutions. Both methods of solving equation 16 produce similar results.

In the first iteration of the algorithm in the simple example there are no pathways to split. See section 2.10 for an example of how to split pathways into sub-pathways.

230 2.9 Re-computation of variables

The variables $[[m_{ik}]]$, $[p_i]$, and $[d_i]$ are recomputed using the definitions presented in table 1 to match the information from the new pathways formed in the above steps. This re-computation is done after deleting pathways and after splitting pathways into sub-pathways.

In the simple example, this re-computation results in the following values for $[[m_{ik}]]$, $[p_i]$, and $[d_i]$:

$$[[m_{ik}]] = \sum_{j=1}^5 \begin{pmatrix} -1 & 1 & -1 & 0 & 0 \\ -1 & -2 & 1 & 1 & 1 \\ 1 & 0 & 1 & -1 & -1 \\ 1 & 0 & 0 & 0 & 0 \\ 0 & 0 & -1 & 1 & -1 \\ 0 & 0 & 0 & 0 & 1 \end{pmatrix} \begin{pmatrix} 1 & 0 & 0 & 0 & 0 & 0 \\ 0 & 1 & 0 & 0 & 0 & 0 \\ 0 & 0 & 1 & 0 & 1 & 0 \\ 0 & 0 & 0 & 0 & 1 & 1 \\ 0 & 0 & 0 & 1 & 0 & 1 \end{pmatrix} = \begin{pmatrix} -1 & 1 & -1 & 0 & -1 & 0 \\ -1 & -2 & 1 & 1 & 2 & 2 \\ 1 & 0 & 1 & -1 & 0 & -2 \\ 1 & 0 & 0 & 0 & 0 & 0 \\ 0 & 0 & -1 & -1 & 0 & 0 \\ 0 & 0 & 0 & 1 & 0 & 1 \end{pmatrix} \begin{matrix} P_1 \\ P_2 \\ P_3 \\ P_4 \\ P_5 \\ P_6 \end{matrix} \begin{matrix} S_1 \\ S_2 \\ S_3 \\ S_4 \\ S_5 \\ S_6 \end{matrix} \quad (19)$$

$$[p_i] = \begin{bmatrix} 0 & 0 & [\tilde{p}_i] & 0 & 0 & 0 \end{bmatrix} + \sum_{k=1}^6 \begin{pmatrix} 0 & 1 & 0 & 0 & 0 & 0 \\ 0 & 0 & 1 & 1 & 2 & 2 \\ 1 & 0 & 1 & 0 & 0 & 0 \\ 1 & 0 & 0 & 0 & 0 & 0 \\ 0 & 0 & 0 & 0 & 0 & 0 \\ 0 & 0 & 0 & 1 & 0 & 1 \end{pmatrix} \begin{pmatrix} 0.1 \\ 0.6 \\ 0.75 \\ 0.75 \\ 0.25 \\ 0.25 \end{pmatrix} = \begin{bmatrix} S_1 & S_2 & S_3 & S_4 & S_5 & S_6 \\ 0.6 & 2.5 & 0.85 & 0.1 & 0 & 1 \end{bmatrix} \text{ ppb/h} \quad (20)$$

$$[d_i] = \begin{bmatrix} 0 & 0 & [\tilde{d}_i] & 0 & 0 & 0 \end{bmatrix} + \sum_{k=1}^6 \begin{pmatrix} 1 & 0 & 1 & 0 & 1 & 0 \\ 1 & 2 & 0 & 0 & 0 & 0 \\ 0 & 0 & 0 & 1 & 0 & 2 \\ 0 & 0 & 0 & 0 & 0 & 0 \\ 0 & 0 & 1 & 1 & 0 & 0 \\ 0 & 0 & 0 & 0 & 0 & 0 \end{pmatrix} \begin{pmatrix} 0.1 \\ 0.6 \\ 0.75 \\ 0.75 \\ 0.25 \\ 0.25 \end{pmatrix} = \begin{bmatrix} S_1 & S_2 & S_3 & S_4 & S_5 & S_6 \\ 1.1 & 1.3 & 1.25 & 0 & 1.5 & 0 \end{bmatrix} \text{ ppb/h} \quad (21)$$

2.10 Second iteration in simple example

240 After the first iteration at the branching point species O in the simple example, we ended up with six pathways (equation 15). The species with the smallest lifetime with respect to these new pathways and the next branching-point species is HO₂ (*S*₃). Looking at the third row of *m_{ik}* in equation 19 (*m_{3k}*), we can see that pathways *P*₄ and *P*₆ destroy HO₂ and pathways *P*₁ and *P*₃ produce HO₂. The connection of these pathways will lead to the formation of 4 new pathways (section 2.4). For example, connecting pathways *P*₆ and *P*₃ we obtain a new pathway *P_n* with the following multiplicities and rates:

$$\begin{aligned}
245 \quad [x_{jn}] &= |m_{36}|[x_{j3}] + m_{33}[x_{j6}] = 2 \cdot [0, 0, 1, 0, 0] + 1 \cdot [0, 0, 0, 1, 1] = [0, 0, 2, 1, 1] \\
f_n &= \frac{f_3 f_6}{\max(p_3, d_3)} = \frac{0.75 \text{ ppb/h} \cdot 0.25 \text{ ppb/h}}{1.25 \text{ ppb/h}} = 0.15 \text{ ppb/h}
\end{aligned} \tag{22}$$

Similarly, the combination of pathways P_1 and P_6 will result in a pathway P_m with multiplicities $[x_{jm}] = [2, 0, 0, 1, 1]$, and a rate $f_m = 0.02 \text{ ppb/h}$. This pathway produces and destroys the number of molecules $[m_{im}] = [-2, 0, 0, 2, 0, 1]$.

At this point there is no production or destruction of HO_2 by deleted pathways, so the rates of connection of existing pathways with deleted pathways $\tilde{f}_e = 0$ (section 2.5). Since the concentration change of the branching-point species HO_2 is
250 $dc_3 = -0.4 \text{ ppb} < 0$, the rates of the pathways destroying HO_2 are redefined to keep the fraction that contributes to dc_3 (section 2.6), and the pathways that produce HO_2 are deleted because they do not contribute to dc_3 (section 2.7).

The rate of the pathway P_m is lower than f_{\min} , so this pathway will be deleted and the variables that store the rates of deleted pathways are updated using equations 14 (section 2.7):

$$\begin{aligned}
[\tilde{r}_j] &= [\tilde{r}_j] + [x_{jm}] \cdot f_m = [0, 0, 0, 0, 0] + [2, 0, 0, 1, 1] \cdot 0.02 \text{ ppb/h} = [0.04, 0, 0, 0.02, 0.02] \text{ ppb/h} \\
[\tilde{p}_i] &= [\tilde{p}_i] + [m_{im}] \cdot f_m = [0, 0, 0, 0, 0, 0] + [0, 0, 0, 2, 0, 1] \cdot 0.02 \text{ ppb/h} = [0, 0, 0, 0.04, 0, 0.02] \text{ ppb/h} \\
[\tilde{d}_i] &= [\tilde{d}_i] + [m_{im}] \cdot f_m = [0, 0, 0, 0, 0, 0] + [2, 0, 0, 0, 0, 0] \cdot 0.02 \text{ ppb/h} = [0.04, 0, 0, 0, 0, 0] \text{ ppb/h}
\end{aligned} \tag{23}$$

255 The next step is to split pathways into sub-pathways (section 2.8). The pathway P_n formed above (equation 22) contains two times reaction R_3 , and one times reactions R_4 and R_5 :



This pathway can be split into two simpler pathways:



In this case, the solution to equation 16 is $[w_e] = [1, 1]$ and $P_n = P_{e1} + P_{e2}$. The sub-pathways have the same rate as the initial pathway because the weights w_e are equal to 1. The sub-pathways P_{e1} and P_{e2} were formed before, when the connection of pathways that produce HO_2 with pathways that destroy HO_2 was made, so their rate is going to be added to the rate of the already existing pathways, and the initial pathway will be deleted from $[[x_{jk}]]$.

265 At the end of this iteration, the variables $[[x_{jk}]]$, $[f_k]$, $[[m_{ik}]]$, $[p_i]$, $[d_i]$, $[\tilde{r}_j]$, $[\tilde{p}_i]$ and $[\tilde{d}_i]$ will have the following form:

$$[[x_{jk}]] = \begin{pmatrix} P_1 & P_2 & P_3 & P_4 & P_5 & P_6 \\ 0 & 0 & 0 & 0 & 1 & 0 \\ 1 & 0 & 0 & 0 & 0 & 0 \\ 0 & 0 & 1 & 0 & 0 & 1 \\ 0 & 0 & 1 & 1 & 0 & 0 \\ 0 & 1 & 0 & 1 & 1 & 1 \end{pmatrix} \begin{matrix} R_1 \\ R_2 \\ R_3 \\ R_4 \\ R_5 \end{matrix} \quad (24)$$

$$[f_k] = \begin{pmatrix} P_1 & P_2 & P_3 & P_4 & P_5 & P_6 \\ 0.6 & 0.24 & 0.4 & 0.08 & 0.06 & 0.6 \end{pmatrix} \text{ ppb/h} \quad (25)$$

$$270 \quad [[m_{ik}]] = \begin{pmatrix} P_1 & P_2 & P_3 & P_4 & P_5 & P_6 \\ 1 & 0 & -1 & 0 & -1 & -1 \\ -2 & 1 & 2 & 2 & 0 & 2 \\ 0 & -1 & 0 & -2 & 0 & 0 \\ 0 & 0 & 0 & 0 & 1 & 0 \\ 0 & -1 & 0 & 0 & -1 & -2 \\ 0 & 1 & 0 & 1 & 1 & 1 \end{pmatrix} \begin{matrix} S_1 \\ S_2 \\ S_3 \\ S_4 \\ S_5 \\ S_6 \end{matrix} \quad (26)$$

$$[p_i] = \begin{pmatrix} S_1 & S_2 & S_3 & S_4 & S_5 & S_6 \\ 0.6 & 2.4 & 0 & 0.1 & 0 & 1 \end{pmatrix} \text{ ppb/h} \quad (27)$$

$$[d_i] = \begin{pmatrix} S_1 & S_2 & S_3 & S_4 & S_5 & S_6 \\ 1.1 & 1.2 & 0.4 & 0. & 1.5 & 0 \end{pmatrix} \text{ ppb/h} \quad (28)$$

275

$$[\tilde{p}_i] = \begin{pmatrix} S_1 & S_2 & S_3 & S_4 & S_5 & S_6 \\ 0 & 0 & 0 & 0.04 & 0 & 0.02 \end{pmatrix} \text{ ppb/h} \quad (29)$$

$$[\tilde{d}_i] = \begin{bmatrix} S_1 & S_2 & S_3 & S_4 & S_5 & S_6 \\ 0.04 & 0 & 0 & 0 & 0 & 0 \end{bmatrix} \text{ ppb/h} \quad (30)$$

$$280 \quad [\tilde{r}_j] = \begin{bmatrix} R_1 & R_2 & R_3 & R_4 & R_5 \\ 0.04 & 0 & 0 & 0.02 & 0.02 \end{bmatrix} \text{ ppb/h} \quad (31)$$

2.11 Final iteration in simple example

The final branching-point species in the simple example is H_2O_2 (S_1). In this final iteration of the algorithm there are six pathways in the matrix $[[x_{jk}]]$ (equation 24). Looking at the first row of $[[m_{ik}]]$ we can see that the pathways P_3 , P_5 and P_6 consume H_2O_2 and the pathway P_1 produces H_2O_2 . The connection of these pathways will lead to the formation of three new pathways.

At this point, the deleted pathways destroy 0.04 H_2O_2 ppb/h (equation 30). This means that we will need to account for the connection of deleted pathways with existing pathways (section 2.5). In this case, the pathway P_1 with rate $f_1 = 0.6$ ppb/h produces one molecule of H_2O_2 . This pathway would have been connected with the deleted pathways at a rate (equation 9):

$$\tilde{f}_1 = \frac{f_1 \tilde{d}_1}{\max(p_1, d_1)} = \frac{0.6 \text{ ppb/h} \cdot 0.04 \text{ ppb/h}}{1.1 \text{ ppb/h}} \approx 0.022 \text{ ppb/h} \quad (32)$$

290 This rate is used to update the variables that store the deleted rates (equation 10):

$$\begin{aligned} [\tilde{r}_j] &= [\tilde{r}_j] + x_{j1} \cdot \tilde{f}_1 = [0.04, 0, 0, 0.02, 0.02] + [0, 1, 0, 0, 0] \cdot 0.022 \text{ ppb/h} \\ &= \begin{bmatrix} R_1 & R_2 & R_3 & R_4 & R_5 \\ 0.04 & 0.022 & 0 & 0.02 & 0.02 \end{bmatrix} \text{ ppb/h} \\ [\tilde{p}_i] &= [\tilde{p}_i] + [m_{i1}] \tilde{f}_1 \quad \text{for } [m_{i1}] > 0 = [0, 0, 0, 0.04, 0, 0.02] + [1, 0, 0, 0, 0, 0] \cdot 0.022 \text{ ppb/h} \\ &= \begin{bmatrix} S_1 & S_2 & S_3 & S_4 & S_5 & S_6 \\ 0.022 & 0 & 0 & 0.04 & 0 & 0.02 \end{bmatrix} \text{ ppb/h} \\ [\tilde{d}_i] &= [\tilde{d}_i] + |[m_{i1}]| \tilde{f}_1 \quad \text{for } [m_{i1}] < 0 = [0.04, 0, 0, 0, 0, 0] + [0, 2, 0, 0, 0, 0] \cdot 0.022 \text{ ppb/h} \\ &= \begin{bmatrix} S_1 & S_2 & S_3 & S_4 & S_5 & S_6 \\ 0.04 & 0.043 & 0 & 0 & 0 & 0 \end{bmatrix} \text{ ppb/h} \end{aligned} \quad (33)$$

After accounting for the connection of deleted and existing pathways, the rates of the pathways P_3 , P_5 and P_6 are redefined because they contribute to the H_2O_2 concentration change $dc_5 = -0.5$ ppb (section 2.6). The pathway P_1 is deleted because it

does not contribute to the H₂O₂ concentration change, one pathway with rate $< f_{\min}$ is deleted (section 2.7), and no pathways
 295 are split into sub-pathways (section 2.8). At the end of this iteration, the variables $[[x_{jk}]]$, $[f_k]$, $[[m_{ik}]]$, $[p_i]$, $[d_i]$, $[\tilde{p}_i]$ and $[\tilde{d}_i]$
 will have the following form:

$$[[x_{jk}]] = \begin{pmatrix} P_1 & P_2 & P_3 & P_4 & P_5 & P_6 \\ 0 & 0 & 0 & 0 & 0 & 0 \\ 0 & 0 & 0 & 0 & 1 & 1 \\ 0 & 1 & 0 & 1 & 1 & 1 \\ 0 & 1 & 1 & 0 & 1 & 0 \\ 1 & 0 & 1 & 1 & 0 & 1 \end{pmatrix} \begin{matrix} R_1 \\ R_2 \\ R_3 \\ R_4 \\ R_5 \end{matrix} \quad (34)$$

$$[f_k] = \begin{matrix} P_1 & P_2 & P_3 & P_4 & P_5 & P_6 \\ \begin{bmatrix} 0.24 & 0.182 & 0.08 & 0.273 & 0.218 & 0.327 \end{bmatrix} \end{matrix} \quad \text{ppb/h} \quad (35)$$

300

$$[[m_{ik}]] = \begin{pmatrix} P_1 & P_2 & P_3 & P_4 & P_5 & P_6 \\ 0 & -1 & 0 & -1 & 0 & 0 \\ 1 & 2 & 2 & 2 & 0 & 0 \\ -1 & 0 & -2 & 0 & 0 & 0 \\ 0 & 0 & 0 & 0 & 0 & 0 \\ -1 & 0 & 0 & -2 & 0 & -2 \\ 1 & 0 & 1 & 1 & 0 & 1 \end{pmatrix} \begin{matrix} S_1 \\ S_2 \\ S_3 \\ S_4 \\ S_5 \\ S_6 \end{matrix} \quad (36)$$

$$[p_i] = \begin{matrix} S_1 & S_2 & S_3 & S_4 & S_5 & S_6 \\ \begin{bmatrix} 0.022 & 1.309 & 0 & 0.1 & 0 & 1.0 \end{bmatrix} \end{matrix} \quad \text{ppb/h} \quad (37)$$

$$305 \quad [d_i] = \begin{matrix} S_1 & S_2 & S_3 & S_4 & S_5 & S_6 \\ \begin{bmatrix} 0.522 & 0.109 & 0.4 & 0 & 1.5 & 0.0 \end{bmatrix} \end{matrix} \quad \text{ppb/h} \quad (38)$$

$$[\tilde{p}_i] = \begin{matrix} S_1 & S_2 & S_3 & S_4 & S_5 & S_6 \\ \begin{bmatrix} 0.022 & 0 & 0 & 0.1 & 0 & 0.08 \end{bmatrix} \end{matrix} \quad \text{ppb/h} \quad (39)$$

$$[\tilde{d}_i] = \begin{bmatrix} S_1 & S_2 & S_3 & S_4 & S_5 & S_6 \\ 0.067 & 0.109 & 0 & 0 & 0.06 & 0.0 \end{bmatrix} \text{ ppb/h} \quad (40)$$

310

$$[\tilde{r}_j] = \begin{bmatrix} R_1 & R_2 & R_3 & R_4 & R_5 \\ 0.1 & 0.055 & 0 & 0.02 & 0.08 \end{bmatrix} \text{ ppb/h} \quad (41)$$

2.12 Calculation of contributions

We calculate the contributions $[C_k]$ of the pathways P_k to the production or destruction of a species S_i as the number of molecules of S_i produced or destroyed by P_k over the number of molecules of S_i produced or destroyed by all pathways:

$$[C_k] = \begin{cases} \frac{[m_{ik}][f_k]}{p_i} & \text{if } P_k \text{ produces } S_i, \\ \frac{[m_{ik}][f_k]}{d_i} & \text{if } P_k \text{ destroys } S_i \end{cases} \quad (42)$$

We use a similar expression to calculate the contribution of deleted pathways to the production or destruction of a species S_i :

$$\begin{aligned} \tilde{C}_p &= \frac{\tilde{p}_i}{p_i} & \text{for deleted pathways producing } S_i, \\ \tilde{C}_d &= \frac{\tilde{d}_i}{d_i} & \text{for deleted pathways destroying } S_i, \end{aligned} \quad (43)$$

320 The expression 42 involves the element-wise multiplication of two vectors. For example, for the species OH in our simple example:

$$\begin{aligned} C_k &= \frac{[m_{3k}][f_k]}{p_3} = \left[\frac{1 \cdot 0.24}{1.309}, \frac{2 \cdot 0.182}{1.309}, \frac{2 \cdot 0.08}{1.309}, \frac{2 \cdot 0.273}{1.309}, \frac{0 \cdot 0.218}{1.309}, \frac{0 \cdot 0.327}{1.309} \right] \frac{\text{ppb/h}}{\text{ppb/h}} \\ &= \begin{bmatrix} P_1 & P_2 & P_3 & P_4 & P_5 & P_6 \\ 0.183 & 0.278 & 0.122 & 0.417 & 0 & 0 \end{bmatrix} \end{aligned} \quad (44)$$

325 Thus, in this simple example the pathway P_4 involving the interaction between reactions R_3 and R_5 is the most important chain of reactions for the production of OH, contributing 41.7% of the OH production (table 2). The interaction between reactions R_3 and R_4 (pathway P_2) is also important, contributing 27.8% of the OH production. Deleted pathways do not contribute to the OH production, but they contribute 100% of the OH destruction ($\tilde{C}_d = \tilde{d}_i/d_i = 0.109/0.109 = 1$). This means

that if we were interested in understanding the chemical reaction chains that destroy OH in this example, we would need to repeat the analysis with a smaller f_{\min} .

In this simple example, it is easy to see that pathways P_4 and P_2 are important for OH production without using the algorithm, but when there are hundreds of reactions interacting the pathway analysis program is a valuable tool to understand the chemical mechanisms that produce the concentration change of a species in an atmospheric chemistry model. Also, even in this simple example we can see how this algorithm provides valuable quantitative information about the contribution of each pathway to the production of a species.

ID	Pathway	Contribution (%)	Rate
P_4	$\text{H}_2\text{O}_2 + \text{O} \longrightarrow \text{OH} + \text{HO}_2$	41.7	0.273
	$\text{HO}_2 + \text{O} \longrightarrow \text{OH} + \text{O}_2$		
	Net: $\text{H}_2\text{O}_2 + 2\text{O} \longrightarrow 2\text{OH} + \text{O}_2$		
P_2	$\text{H}_2\text{O}_2 + \text{O} \longrightarrow \text{OH} + \text{HO}_2$	27.8	0.182
	$\text{HO}_2 + h\nu \longrightarrow \text{OH} + \text{O}$		
	Net: $\text{H}_2\text{O}_2 \longrightarrow 2\text{OH}$		
P_1	$\text{HO}_2 + \text{O} \longrightarrow \text{OH} + \text{O}_2$	18.3	0.24
	Net: $\text{HO}_2 + \text{O} \longrightarrow \text{OH} + \text{O}_2$		
P_3	$\text{HO}_2 + h\nu \longrightarrow \text{OH} + \text{O}$	12.2	0.08
	$\text{HO}_2 + \text{O} \longrightarrow \text{OH} + \text{O}_2$		
	Net: $2\text{HO}_2 \longrightarrow 2\text{OH} + \text{O}_2$		

Table 2: Contribution of pathways to the production of OH in the simple example used to explain the algorithm.

3 Implementation

We implement Lehmann’s (2004) algorithm in Python. We designed an object-oriented code defining a class to store the variables listed in table 1 and separating the steps described in section 2 into different class methods. We run these methods in a main method that performs the loop shown in figure 1. We represent the multiplicities $[[x_{jk}]]$ of the pathways as a sparse matrix to optimize memory usage. Our implementation includes the option to find pathways using multiprocessing to speed up the computation time.

Before the construction of pathways it is essential to ensure the concentration changes of all species are balanced by the reaction’s production and destruction (equation 1). Our implementation does not try to correct for imbalances, but we include a function that displays a warning if mass balance is not fulfilled. The warning is displayed if the unbalance is greater than a relative tolerance of 1×10^{-3} if the concentration change is greater or equal to 1 molecule/ cm^3 , and to an absolute tolerance of 1×10^{-3} if the concentration change is lower than 1 molecule/ cm^3 . We use an absolute tolerance for concentration changes lower than 1 molecule/ cm^3 because we consider that concentration changes lower than 1×10^{-3} molecules/ cm^3 are unim-

345 portant. If this warning is displayed, the model output should be checked for potential problems or corrected (see (Lehmann, 2002)for an example of how to do this).

The code includes several functions that are useful for analyzing the pathways. After the main algorithm loop ends, the variables in table 1 have all the information of the pathways that have been found. The code includes functions to save these variables to binary files and to read them for future analysis. The code also has functions to transform the representation of a pathway from an array of multiplicities to a string, to get the net reaction of a pathway, to create a latex table with the pathways that contribute to the production or destruction of a species of interest, and to assign a unique identifier to each pathway. This identifier is a string containing the multiplicities and the indexes of the reactions in a pathway. The same pathway can be formed multiple times during the algorithm, so we use this identifier to avoid repeating pathways. We also include a function to calculate the contribution of all pathways to the production or destruction of a species.

355 Our implementation includes the option to specify species that will be ignored as branching point species. If we are interested in finding pathways at a specific timescale, it is convenient not to consider species with lifetimes higher than the timescale of interest as branching-points. Our implementation also includes the option to ignore species as branching-points specifying a maximum lifetime of branching-point species.

3.1 Tests

360 The code includes run-time tests to ensure that the code works well. If the construction of pathways is correct, the rates of the reactions must be completely distributed to the pathways:

$$[r_j] = [\tilde{r}_j] + \sum_{k=1}^{n_p} [[x_{jk}]] \cdot [f_k], \quad j = 1 \dots n_r \quad (45)$$

This condition ensures that the number of molecules of a species produced or destroyed by the initial reactions is the same as the number of molecules produced or destroyed by the pathways. The code checks that equation 45 is fulfilled in each iteration of the algorithm, and displays a warning if it is not satisfied.

The code also includes unit tests to ensure that the code works as expected in a simple scenario with four reactions representing Chapman’s O₃ destruction mechanism (Chapman, 1930). This scenario is used by Lehmann (2004) to explain how the algorithm works. We include tests to ensure that our implementation finds the same pathways and rates as those found by Lehmann (2004) in this very simple example.

370 3.2 Using Chempath

Chempath is available at <https://github.com/DanyIvan/chempath>. This code repository includes a tutorial on how to use Chempath, as well as some examples of how to apply Chempath to a box model and to a one-dimensional photochemical model (section 4).

There are two important steps to use Chempath. First, the user needs to transform the output of a photochemical model into files readable by Chempath. The code repository includes some examples of how to create these input files. Second, the user

needs to choose a minimum rate of pathways f_{\min} . This can be done by trial and error, or setting it as a fraction of the rate of total production or destruction by the reactions of the species the user is interested in finding pathways for. However, this way of setting f_{\min} might still require further trial and error to find an appropriate fraction of the total production or destruction by all reactions. Ideally, f_{\min} will be small enough so that the deleted pathways do not contribute significantly to the production
 380 or destruction of a species of interest. However, if f_{\min} is too small, the code might take a long time to run.

4 Application example: Pathways in a one-dimensional photochemical model

In this section, we show how to apply *Chempath* to the one-dimensional photochemical model *photochem* (Wogan et al. 2023, <https://github.com/Nicholaswogan/photochem>). We run the *photochem* model with the “Modern Earth” reaction scheme that includes 1281 reactions between 113 species. We run the model to photochemical equilibrium using surface flux boundary
 385 conditions for O_2 , CH_4 , CO , and H_2 . We choose fluxes of 3.3×10^{11} , 5×10^{10} , 1.2×10^8 and 3×10^9 molecules/ cm^2/s for each of these species respectively. The choice of these fluxes is arbitrary and motivated to get similar conditions to the present atmosphere. For all other species, we use the default boundary conditions of the “Modern Earth” reaction scheme. After the model reaches equilibrium, we decrease the O_2 surface flux to 2.5×10^{11} molecules/ cm^2/s and run the model for 5 million years. The idea behind the reduction of the O_2 surface flux is to create a perturbation that causes concentration changes to
 390 explore with *Chempath*. The concentration of O_2 in the model is controlled mainly by the surface flux and by oxidation of reduced species like CH_4 , CO and H_2 in a timescale of millions of years (the estimated lifetime for O_2 in the modern atmosphere is ~ 2 million years (Kasting, 2013)). The *photochem* model uses a solver with an adaptive timestep (CVODE BDF method created by Sundials Computing). In our simulation the timestep varies from $10^{-5}s$ to $10^{12}s$. We only output the model results when the simulation time is greater than 10^{11} s.

395 The model output shows that O_2 and O_3 concentrations tend to decrease at all altitudes as a consequence of the decrease in the O_2 surface input flux (figure 2). It is clear that this O_3 concentration decrease is a consequence of the decrease in the O_2 surface input flux, but if we want to know what are the chemical mechanisms that explain the O_3 concentration change, we need to use the pathway analysis program. We apply *Chempath* to the *photochem* model output to gain insight into the chemical reaction chains that produce and destroy O_3 in this model run.

400 4.1 Methods: How to find pathways in the *photochem* model

The application of *Chempath* to the *photochem* model output requires the calculation of vertical transport supply or removal terms. The *photochem* model calculates the concentration changes of long-lived species solving the equation:

$$\frac{\partial f_i}{\partial t} = \frac{1}{\rho} \frac{\partial}{\partial z} \Phi_i + \frac{\Pi_i}{\rho} - \frac{L_i}{\rho} - \frac{\Omega_i}{\rho}, \quad (46)$$

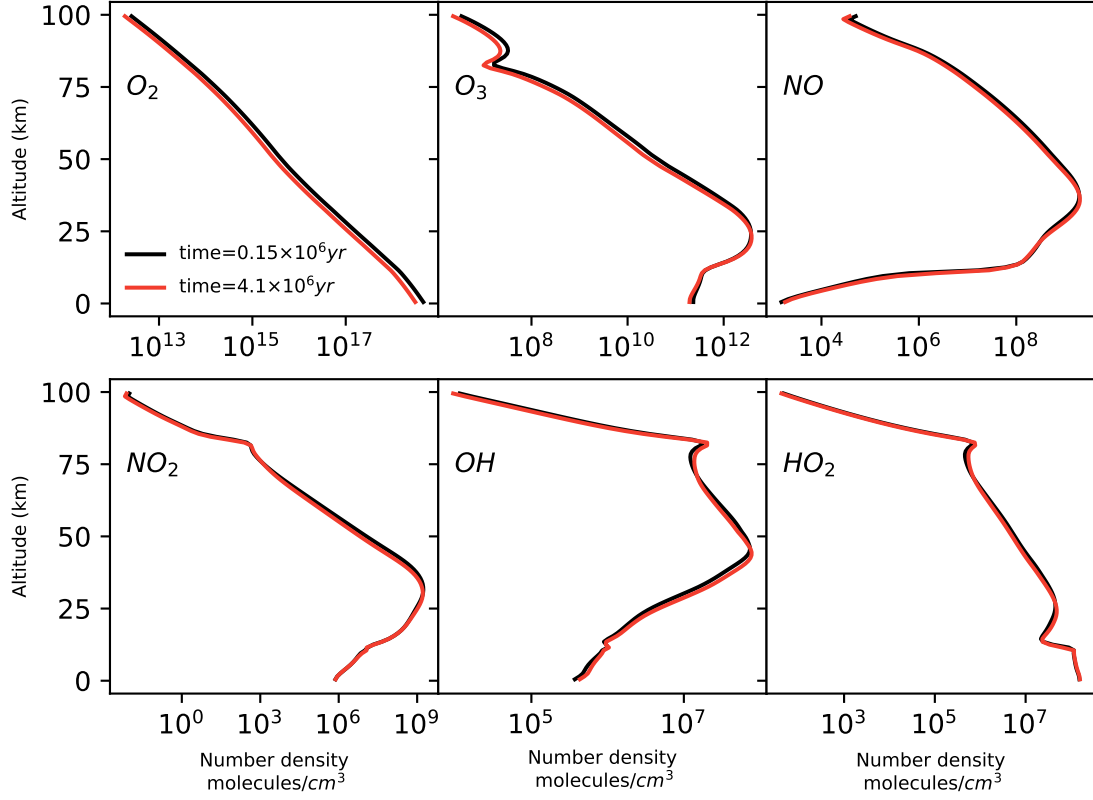


Figure 2. Number density profiles of O_2 , O_3 , NO , NO_2 , OH and HO_2 calculated by the *photochem* model at time= 0.15 million years (black line) and at time= 4.1 million years (red line). In this model run we decrease the O_2 input surface flux. As a result, the O_2 and O_3 number densities tend to decrease at all altitudes. The concentration of NO , NO_2 , OH and HO_2 decrease and increase at different altitudes.

where f_i is the mixing ratio of species i , ρ is the total number density, z is altitude, Π_i and D_i are the chemical production and destruction of species i , Φ_i is the vertical transport flux of species i , and Ω_i is the destruction of species i from rainout (see Wogan et al. 2022 for more details). We assume that ρ is constant over time and that equation 46 can be represented as :

$$\frac{d\rho_i}{dt} = \Pi_i - D_i - \Omega_i + T_i, \quad (47)$$

where ρ_i is the number density of species i and T_i is the supply or removal of species i by the vertical transport . We obtain Π_i , D_i , and Ω_i from the *photochem* model output and use equation 47 to calculate T_i at a given altitude.

To incorporate the effect of vertical transport and rainout into the pathway analysis program we add the following pseudo-reactions to the reaction system for each species S_i :

$$\begin{aligned}
S_i &\longrightarrow S_{i,\text{trpt}} \text{ if transport removes } S_i \\
S_{i,\text{trpt}} &\longrightarrow S_i \text{ if transport supplies } S_i \\
S_i &\longrightarrow S_{i,\text{rainout}},
\end{aligned}
\tag{48}$$

The rate of these pseudo-reactions is given by the transport rates calculated from equation 47 and the rainout rates calculated by the model.

415 We run *Chempath* with the updated reaction system at each altitude grid and at 40 time points distributed across the model run. We prescribe a variable minimum pathway rate f_{\min} that we calculate as the minimum of the chemical production by reactions (including transport pseudo-reactions) of O_2 , O_3 , CO , H_2 and CH_4 divided by 1000. We use these species to calculate f_{\min} because we are interested in understanding their concentration changes. We do not consider these species as branching-points. We also ignore N_2 , CO_2 , and H_2O as branching-point species, treating them as long-lived inert species.

420 Our f_{\min} choice keeps the contribution of deleted pathways to O_3 production and destruction below 5% at all altitudes and times in our analysis. The number of reactions with rate $> f_{\min}$ varies with altitude, and ranges from 78 to 132.

4.2 Results: Ozone destruction and production pathways in the *photochem* model

Chempath allows us to identify the most important pathways for O_3 production and destruction at a given altitude and time in our *photochem* model run (figures 3 and 4, and table 3).

425 In the troposphere (below 11 km in our model run), O_3 production in the *photochem* model is dominated by transport (pathway $P_{2.1}$) and by the photochemical oxidation of hydrocarbons, including methane and the methylperoxy radical (pathways $P_{2.2}$ to $P_{2.4}$) under the presence of nitrogen oxide radicals (NO_x). These hydrocarbon oxidation pathways are similar to the “smog mechanism” that produces tropospheric O_3 through oxidation of hydrocarbons (Haagen-Smit, 1952; A. Volz-Thomas, 1994). The tropospheric O_3 destruction is dominated by O_3 photolysis and subsequent CH_4 oxidation under the presence of
430 hydrogen oxide radicals (HO_x , pathways $D_{2.1}$ and $D_{2.2}$). Ozone loss catalyzed by HO_x radicals is also important (pathway $D_{2.3}$).

In the stratosphere (11-50km), O_3 production is mainly occurring via CO and CH_4 oxidation under the presence of NO_x radicals below 25km (pathways $P_{2.6}$ and $P_{2.7}$), and by the Chapman production pathway $P_{2.8}$ above 25km. The main stratospheric O_3 destruction mechanisms involve transport (pathway $D_{2.4}$), Chapman-like destruction pathways ($D_{2.5}$, $D_{2.11}$), and
435 destruction by HO_x and NO_x radicals (pathways $D_{2.3}$ and $D_{2.6}$ to $D_{2.10}$). Catalytic cycles involving NO_x and HO_x radicals are important for stratospheric O_3 destruction (Lary, 1997; Jacob, 1999). *Chempath* can identify these well-known catalytic cycles.

Above 50km of altitude, the main O_3 production mechanisms are Chapman-like production pathways ($P_{2.8}$ to $P_{2.11}$), and the main O_3 destruction mechanisms involve O_3 photolysis coupled to HO_x radicals cycles (pathways $D_{2.12}$ and $D_{2.13}$),
440 destruction by HO_x radicals (pathways $D_{2.14}$ to $D_{2.17}$), and Chapman-like destruction pathways ($P_{2.18}$).

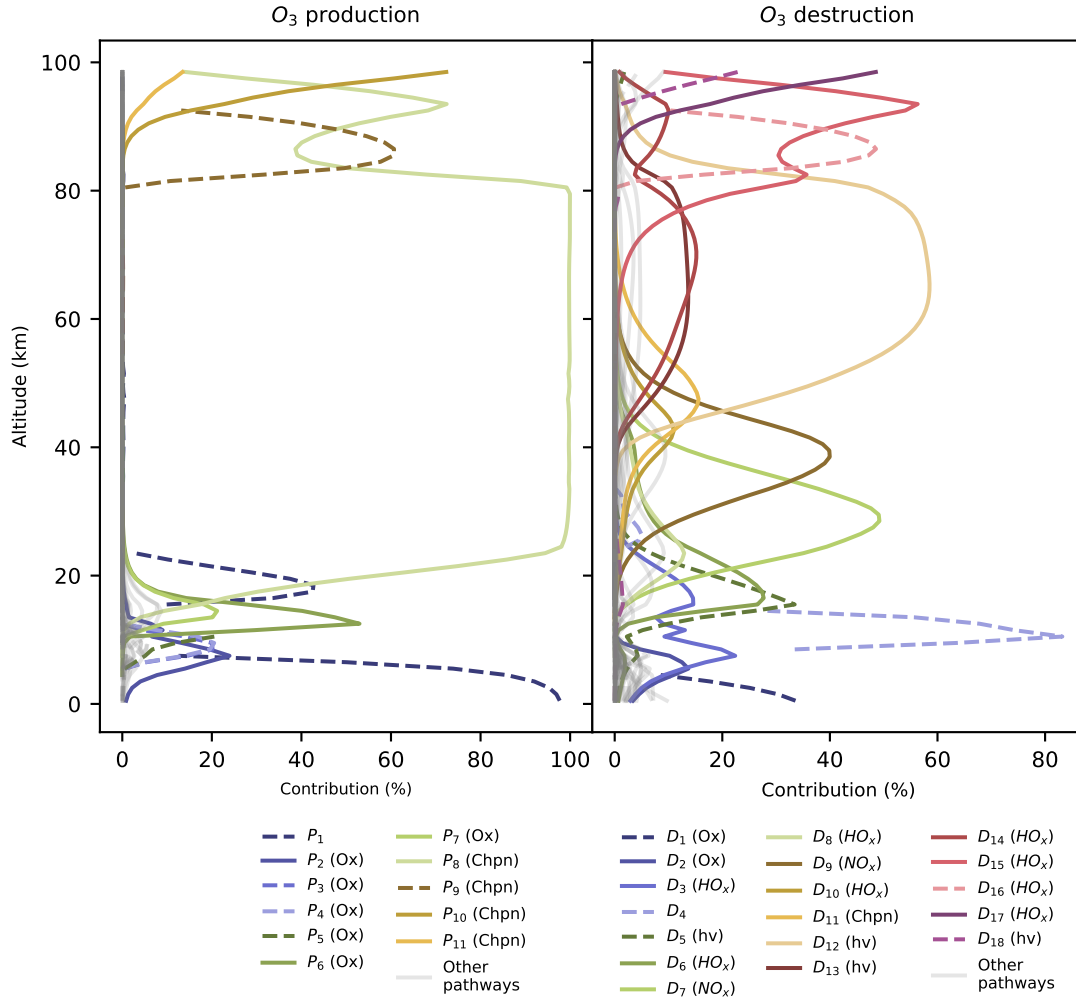


Figure 3. Contribution of pathways to O_3 production and destruction as a function of altitude at the model time= 4.1 million years. The main pathways are plotted in color and the less important pathways are plotted in gray. Pathways that include transport pseudo-reactions are plotted in dashed lines. These pathways show discontinuities because transport can either supply or remove O_3 at different altitudes. The symbols in the legend group the pathways into five categories: Oxidation (Ox), Chapman-like (Chpn), photolysis (hv), hydrogen oxide (HO_x), and nitrogen oxide (NO_x) pathways. The pathways are listed in table 3.

The contribution profiles shown in figure 3 have a similar structure in all the time steps we analyzed. For example, at 30km of altitude, the pathways producing and destroying O₃ have very similar contributions over time (figure 4). Consequently, the pathways shown in figure 3 and listed in table 3 are a good representation of the pathways that produce and destroy O₃ across all times we analyzed. These pathways are similar to those found in a previous study of chemical pathways affecting O₃ in the atmosphere (Grenfell et al., 2006).

ID	Pathway	Maximum contribution %	Rate $\frac{\text{molecules}}{\text{cm}^2 \text{ s}}$	Altitude of maximum contribution km
P_1	$\text{O}_{3\text{trpt}} \longrightarrow \text{O}_3$ Net: $\text{O}_{3\text{trpt}} \longrightarrow \text{O}_3$	97.677	8.501e+04	0.5
P_2	$2(\text{CH}_4 + \text{OH} \longrightarrow \text{CH}_3 + \text{H}_2\text{O})$ $2(\text{CH}_3 + \text{O}_2 + \text{M} \longrightarrow \text{CH}_3\text{O}_2 + \text{M})$ $2(\text{CH}_3\text{O}_2 + \text{NO} \longrightarrow \text{CH}_3\text{O} + \text{NO}_2)$ $2(\text{NO}_2 + h\nu \longrightarrow \text{NO} + \text{O})$ $2(\text{CH}_3\text{O} + \text{O}_2 \longrightarrow \text{H}_2\text{CO} + \text{HO}_2)$ $2(\text{H}_2\text{CO} + h\nu \longrightarrow \text{CO} + \text{H}_2)$ $\text{HO}_2 + \text{HO}_2 \longrightarrow \text{H}_2\text{O}_2 + \text{O}_2$ $\text{H}_2\text{O}_2 + h\nu \longrightarrow \text{OH} + \text{OH}$ $2(\text{O} + \text{O}_2 + \text{M} \longrightarrow \text{O}_3 + \text{M})$ Net: $5\text{O}_2 + 2\text{CH}_4 \longrightarrow 2\text{H}_2 + 2\text{H}_2\text{O} + 2\text{CO} + 2\text{O}_3$	23.943	3.430e+03	7.5
P_3	$4(\text{CH}_3\text{O}_{2\text{trpt}} \longrightarrow \text{CH}_3\text{O}_2)$ $4(\text{CH}_3\text{O}_2 + \text{NO} \longrightarrow \text{CH}_3\text{O} + \text{NO}_2)$ $4(\text{NO}_2 + h\nu \longrightarrow \text{NO} + \text{O})$ $4(\text{CH}_3\text{O} + \text{O}_2 \longrightarrow \text{H}_2\text{CO} + \text{HO}_2)$ $4(\text{H}_2\text{CO} + h\nu \longrightarrow \text{CO} + \text{H}_2)$ $3(\text{HO}_2 + \text{HO}_2 \longrightarrow \text{H}_2\text{O}_2 + \text{O}_2)$ $2(\text{H}_2\text{O}_2 + \text{OH} \longrightarrow \text{HO}_2 + \text{H}_2\text{O})$ $\text{H}_2\text{O}_2 + h\nu \longrightarrow \text{OH} + \text{OH}$ $4(\text{O} + \text{O}_2 + \text{M} \longrightarrow \text{O}_3 + \text{M})$ Net: $5\text{O}_2 + 4\text{CH}_3\text{O}_{2\text{trpt}} \longrightarrow 4\text{H}_2 + 2\text{H}_2\text{O} + 4\text{CO} + 4\text{O}_3$	20.146	1.726e+03	8.5

P_4	$4(\text{CH}_3\text{O}_{2\text{trpt}} \longrightarrow \text{CH}_3\text{O}_2)$ $4(\text{CH}_3\text{O}_2 + \text{NO} \longrightarrow \text{CH}_3\text{O} + \text{NO}_2)$ $4(\text{NO}_2 + h\nu \longrightarrow \text{NO} + \text{O})$ $4(\text{CH}_3\text{O} + \text{O}_2 \longrightarrow \text{H}_2\text{CO} + \text{HO}_2)$ $4(\text{H}_2\text{CO} + h\nu \longrightarrow \text{CO} + \text{H}_2)$ $2(\text{OH} + \text{HO}_2 \longrightarrow \text{H}_2\text{O} + \text{O}_2)$ $\text{HO}_2 + \text{HO}_2 \longrightarrow \text{H}_2\text{O}_2 + \text{O}_2$ $\text{H}_2\text{O}_2 + h\nu \longrightarrow \text{OH} + \text{OH}$ $4(\text{O} + \text{O}_2 + \text{M} \longrightarrow \text{O}_3 + \text{M})$ Net: $5\text{O}_2 + 4\text{CH}_3\text{O}_{2\text{trpt}} \longrightarrow 4\text{H}_2 + 2\text{H}_2\text{O} + 4\text{CO} + 4\text{O}_3$	20.519	2.457e+03	9.5
P_5	$2(\text{CH}_3\text{O}_{2\text{trpt}} \longrightarrow \text{CH}_3\text{O}_2)$ $2(\text{CH}_3\text{O}_2 + \text{NO} \longrightarrow \text{CH}_3\text{O} + \text{NO}_2)$ $2(\text{NO}_2 + h\nu \longrightarrow \text{NO} + \text{O})$ $2(\text{CH}_3\text{O} + \text{O}_2 \longrightarrow \text{H}_2\text{CO} + \text{HO}_2)$ $2(\text{H}_2\text{CO} + h\nu \longrightarrow \text{CO} + \text{H}_2)$ $\text{HO}_2 + \text{HO}_2 \longrightarrow \text{H}_2\text{O}_2 + \text{O}_2$ $\text{H}_2\text{O}_2 \longrightarrow \text{H}_2\text{O}_{2\text{trpt}}$ $2(\text{O} + \text{O}_2 + \text{M} \longrightarrow \text{O}_3 + \text{M})$ Net: $3\text{O}_2 + 2\text{CH}_3\text{O}_{2\text{trpt}} \longrightarrow 2\text{H}_2 + 2\text{CO} + 2\text{O}_3 + \text{H}_2\text{O}_{2\text{trpt}}$	20.548	7.345e+03	10.5
P_6	$\text{CO} + \text{OH} \longrightarrow \text{CO}_2 + \text{H}$ $\text{H} + \text{O}_2 + \text{M} \longrightarrow \text{HO}_2 + \text{M}$ $\text{NO} + \text{HO}_2 \longrightarrow \text{NO}_2 + \text{OH}$ $\text{NO}_2 + h\nu \longrightarrow \text{NO} + \text{O}$ $\text{O} + \text{O}_2 + \text{M} \longrightarrow \text{O}_3 + \text{M}$ Net: $2\text{O}_2 + \text{CO} \longrightarrow \text{CO}_2 + \text{O}_3$	52.975	1.379e+04	12.5
P_7	$\text{CH}_4 + \text{OH} \longrightarrow \text{CH}_3 + \text{H}_2\text{O}$ $\text{CH}_3 + \text{O}_2 + \text{M} \longrightarrow \text{CH}_3\text{O}_2 + \text{M}$ $\text{CH}_3\text{O}_2 + \text{NO} \longrightarrow \text{CH}_3\text{O} + \text{NO}_2$ $2(\text{NO}_2 + h\nu \longrightarrow \text{NO} + \text{O})$ $\text{CH}_3\text{O} + \text{O}_2 \longrightarrow \text{H}_2\text{CO} + \text{HO}_2$ $\text{H}_2\text{CO} + h\nu \longrightarrow \text{CO} + \text{H}_2$ $\text{NO} + \text{HO}_2 \longrightarrow \text{NO}_2 + \text{OH}$ $2(\text{O} + \text{O}_2 + \text{M} \longrightarrow \text{O}_3 + \text{M})$ Net: $4\text{O}_2 + \text{CH}_4 \longrightarrow \text{H}_2 + \text{H}_2\text{O} + \text{CO} + 2\text{O}_3$	21.181	2.425e+03	14.5

P_8	$\text{O}_2 + h\nu \longrightarrow \text{O} + \text{O}$ $2(\text{O} + \text{O}_2 + \text{M} \longrightarrow \text{O}_3 + \text{M})$ $\text{Net: } 3\text{O}_2 \longrightarrow 2\text{O}_3$	99.959	8.865e+04	79.5
P_9	$\text{O}_{\text{trpt}} \longrightarrow \text{O}$ $\text{O} + \text{O}_2 + \text{M} \longrightarrow \text{O}_3 + \text{M}$ $\text{Net: } \text{O}_2 + \text{O}_{\text{trpt}} \longrightarrow \text{O}_3$	60.679	2.850e+05	86.5
P_{10}	$\text{O}_2 + h\nu \longrightarrow \text{O} + \text{O}(^1\text{D})$ $\text{O}(^1\text{D}) + \text{N}_2 \longrightarrow \text{O} + \text{N}_2$ $2(\text{O} + \text{O}_2 + \text{M} \longrightarrow \text{O}_3 + \text{M})$ $\text{Net: } 3\text{O}_2 \longrightarrow 2\text{O}_3$	72.342	1.613e+04	98.5
P_{11}	$\text{O}_2 + h\nu \longrightarrow \text{O} + \text{O}(^1\text{D})$ $\text{O}(^1\text{D}) + \text{O}_2 \longrightarrow \text{O} + \text{O}_2$ $2(\text{O} + \text{O}_2 + \text{M} \longrightarrow \text{O}_3 + \text{M})$ $\text{Net: } 3\text{O}_2 \longrightarrow 2\text{O}_3$	13.452	3.000e+03	98.5
D_1	$\text{O}_3 + h\nu \longrightarrow \text{O}(^1\text{D}) + \text{O}_2$ $\text{O}(^1\text{D}) + \text{H}_2\text{O} \longrightarrow \text{OH} + \text{OH}$ $2(\text{CH}_4 + \text{OH} \longrightarrow \text{CH}_3 + \text{H}_2\text{O})$ $2(\text{CH}_3 + \text{O}_2 + \text{M} \longrightarrow \text{CH}_3\text{O}_2 + \text{M})$ $2(\text{CH}_3\text{O}_2 \longrightarrow \text{CH}_3\text{O}_{2\text{trpt}})$ $\text{Net: } \text{O}_2 + 2\text{CH}_4 + \text{O}_3 \longrightarrow \text{H}_2\text{O} + 2\text{CH}_3\text{O}_{2\text{trpt}}$	33.608	2.925e+04	0.5
D_2	$2(\text{O}_3 + h\nu \longrightarrow \text{O} + \text{O}_2)$ $2(\text{CH}_4 + \text{OH} \longrightarrow \text{CH}_3 + \text{H}_2\text{O})$ $2(\text{CH}_3 + \text{O}_2 + \text{M} \longrightarrow \text{CH}_3\text{O}_2 + \text{M})$ $2(\text{CH}_3\text{O}_2 + \text{O} \longrightarrow \text{CH}_3\text{O} + \text{O}_2)$ $2(\text{CH}_3\text{O} + \text{O}_2 \longrightarrow \text{H}_2\text{CO} + \text{HO}_2)$ $2(\text{H}_2\text{CO} + h\nu \longrightarrow \text{CO} + \text{H}_2)$ $\text{HO}_2 + \text{HO}_2 \longrightarrow \text{H}_2\text{O}_2 + \text{O}_2$ $\text{H}_2\text{O}_2 + h\nu \longrightarrow \text{OH} + \text{OH}$ $\text{Net: } 2\text{CH}_4 + 2\text{O}_3 \longrightarrow 2\text{H}_2 + 2\text{H}_2\text{O} + \text{O}_2 + 2\text{CO}$	13.697	2.866e+03	5.5
D_3	$\text{HO}_2 + \text{HO}_2 \longrightarrow \text{H}_2\text{O}_2 + \text{O}_2$ $\text{H}_2\text{O}_2 + h\nu \longrightarrow \text{OH} + \text{OH}$ $2(\text{OH} + \text{O}_3 \longrightarrow \text{HO}_2 + \text{O}_2)$ $\text{Net: } 2\text{O}_3 \longrightarrow 3\text{O}_2$	22.404	3.210e+03	7.5

D_4	$\text{O}_3 \longrightarrow \text{O}_{3\text{trpt}}$ $\text{Net: O}_3 \longrightarrow \text{O}_{3\text{trpt}}$	83.208	5.948e+04	10.5
D_5	$\text{O}_3 + h\nu \longrightarrow \text{O} + \text{O}_2$ $\text{O} \longrightarrow \text{O}_{\text{trpt}}$ $\text{Net: O}_3 \longrightarrow \text{O}_2 + \text{O}_{\text{trpt}}$	33.453	8.377e+03	15.5
D_6	$\text{O}_3 + h\nu \longrightarrow \text{O}(^1\text{D}) + \text{O}_2$ $\text{O}(^1\text{D}) + \text{H}_2\text{O} \longrightarrow \text{OH} + \text{OH}$ $\text{OH} + \text{HO}_2 \longrightarrow \text{H}_2\text{O} + \text{O}_2$ $\text{OH} + \text{O}_3 \longrightarrow \text{HO}_2 + \text{O}_2$ $\text{Net: } 2\text{O}_3 \longrightarrow 3\text{O}_2$	27.694	5.007e+03	16.5
D_7	$\text{O}_3 + h\nu \longrightarrow \text{O} + \text{O}_2$ $\text{NO}_2 + \text{O} \longrightarrow \text{NO} + \text{O}_2$ $\text{NO} + \text{O}_3 \longrightarrow \text{NO}_2 + \text{O}_2$ $\text{Net: } 2\text{O}_3 \longrightarrow 3\text{O}_2$	49.204	3.714e+05	28.5
D_8	$\text{O}_3 + h\nu \longrightarrow \text{O} + \text{O}_2$ $\text{HO}_2 + \text{O} \longrightarrow \text{OH} + \text{O}_2$ $\text{OH} + \text{O}_3 \longrightarrow \text{HO}_2 + \text{O}_2$ $\text{Net: } 2\text{O}_3 \longrightarrow 3\text{O}_2$	12.92	1.980e+04	23.5
D_9	$\text{O}_3 + h\nu \longrightarrow \text{O}(^1\text{D}) + \text{O}_2$ $\text{O}(^1\text{D}) + \text{N}_2 \longrightarrow \text{O} + \text{N}_2$ $\text{NO}_2 + \text{O} \longrightarrow \text{NO} + \text{O}_2$ $\text{NO} + \text{O}_3 \longrightarrow \text{NO}_2 + \text{O}_2$ $\text{Net: } 2\text{O}_3 \longrightarrow 3\text{O}_2$	39.97	9.662e+05	38.5
D_{10}	$\text{O}_3 + h\nu \longrightarrow \text{O}(^1\text{D}) + \text{O}_2$ $\text{O}(^1\text{D}) + \text{N}_2 \longrightarrow \text{O} + \text{N}_2$ $\text{HO}_2 + \text{O} \longrightarrow \text{OH} + \text{O}_2$ $\text{OH} + \text{O}_3 \longrightarrow \text{HO}_2 + \text{O}_2$ $\text{Net: } 2\text{O}_3 \longrightarrow 3\text{O}_2$	10.943	2.328e+05	42.5
D_{11}	$\text{O}_3 + h\nu \longrightarrow \text{O}(^1\text{D}) + \text{O}_2$ $\text{O}(^1\text{D}) + \text{N}_2 \longrightarrow \text{O} + \text{N}_2$ $\text{O} + \text{O}_3 \longrightarrow \text{O}_2 + \text{O}_2$ $\text{Net: } 2\text{O}_3 \longrightarrow 3\text{O}_2$	15.596	2.307e+05	47.5

D_{12}	$2(\text{O}_3 + h\nu \longrightarrow \text{O}(^1\text{D}) + \text{O}_2)$ $2(\text{O}(^1\text{D}) + \text{N}_2 \longrightarrow \text{O} + \text{N}_2)$ $\text{O} + \text{OH} \longrightarrow \text{O}_2 + \text{H}$ $\text{HO}_2 + \text{O} \longrightarrow \text{OH} + \text{O}_2$ $\text{H} + \text{O}_2 + \text{M} \longrightarrow \text{HO}_2 + \text{M}$ Net: $2\text{O}_3 \longrightarrow 3\text{O}_2$	58.521	2.554e+05	65.5
D_{13}	$2(\text{O}_3 + h\nu \longrightarrow \text{O}(^1\text{D}) + \text{O}_2)$ $2(\text{O}(^1\text{D}) + \text{O}_2 \longrightarrow \text{O} + \text{O}_2)$ $\text{HO}_2 + \text{O} \longrightarrow \text{OH} + \text{O}_2$ $\text{O} + \text{OH} \longrightarrow \text{O}_2 + \text{H}$ $\text{H} + \text{O}_2 + \text{M} \longrightarrow \text{HO}_2 + \text{M}$ Net: $2\text{O}_3 \longrightarrow 3\text{O}_2$	13.672	6.625e+04	63.5
D_{14}	$\text{O}_3 + h\nu \longrightarrow \text{O}(^1\text{D}) + \text{O}_2$ $\text{O}(^1\text{D}) + \text{N}_2 \longrightarrow \text{O} + \text{N}_2$ $\text{O} + \text{OH} \longrightarrow \text{O}_2 + \text{H}$ $\text{H} + \text{O}_3 \longrightarrow \text{OH} + \text{O}_2$ Net: $2\text{O}_3 \longrightarrow 3\text{O}_2$	15.18	4.997e+04	70.5
D_{15}	$\text{O}_2 + h\nu \longrightarrow \text{O} + \text{O}$ $2(\text{O} + \text{OH} \longrightarrow \text{O}_2 + \text{H})$ $2(\text{H} + \text{O}_3 \longrightarrow \text{OH} + \text{O}_2)$ Net: $2\text{O}_3 \longrightarrow 3\text{O}_2$	56.315	5.890e+04	93.5
D_{16}	$\text{O}_{\text{trpt}} \longrightarrow \text{O}$ $\text{O} + \text{OH} \longrightarrow \text{O}_2 + \text{H}$ $\text{H} + \text{O}_3 \longrightarrow \text{OH} + \text{O}_2$ Net: $\text{O}_3 + \text{O}_{\text{trpt}} \longrightarrow 2\text{O}_2$	48.573	2.281e+05	86.5
D_{17}	$\text{O}_2 + h\nu \longrightarrow \text{O} + \text{O}(^1\text{D})$ $\text{O}(^1\text{D}) + \text{N}_2 \longrightarrow \text{O} + \text{N}_2$ $2(\text{O} + \text{OH} \longrightarrow \text{O}_2 + \text{H})$ $2(\text{H} + \text{O}_3 \longrightarrow \text{OH} + \text{O}_2)$ Net: $2\text{O}_3 \longrightarrow 3\text{O}_2$	48.536	1.082e+04	98.5
D_{18}	$\text{O}_3 + h\nu \longrightarrow \text{O}(^1\text{D}) + \text{O}_2$ $\text{O}(^1\text{D}) + \text{N}_2 \longrightarrow \text{O} + \text{N}_2$ $\text{O} \longrightarrow \text{O}_{\text{trpt}}$ Net: $\text{O}_3 \longrightarrow \text{O}_2 + \text{O}_{\text{trpt}}$	22.849	1.019e+04	98.5

Table 3: Pathways producing and destroying O_3 at time= 4.5 million years of the model run. The contribution profiles of these pathways are shown in figure 3. The contributions and rates in this table correspond to the height at which the pathways contribute the most to O_3 production and destruction. Our algorithm does not yet have the functionality to automatically order the reactions in a pathway to easily follow the flow of molecules. We ordered the reactions in all the pathways in this table by hand.

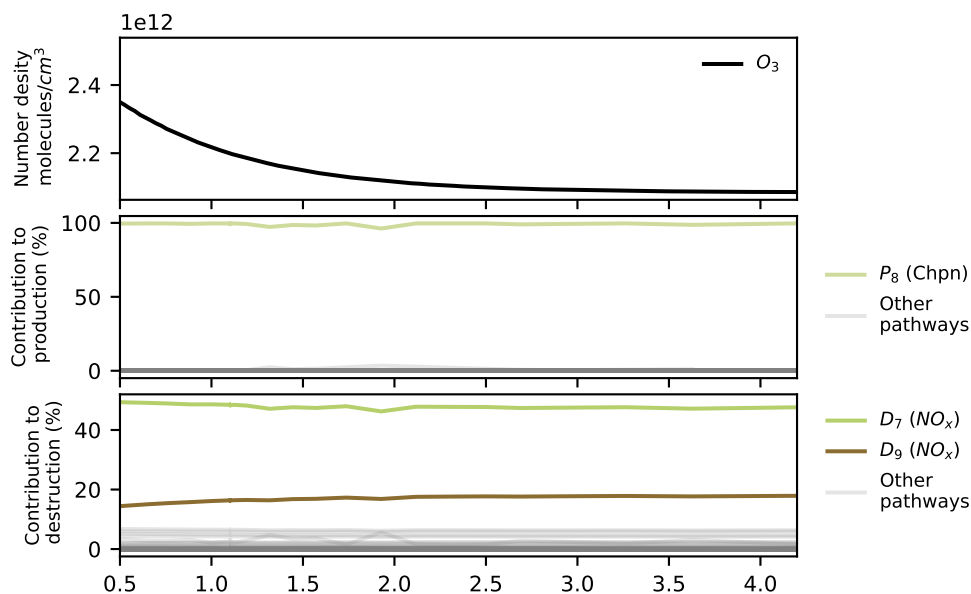


Figure 4. Contributions of the main pathways producing (middle panel) and destroying (bottom panel) O_3 as a function of time at a 30km altitude. The pathways are listed in table 3. The time evolution of the O_3 number density at 30km is shown in the top panel.

4.3 Discussion

The application of Chempath can lead to the detection of unexpected pathways in a model run. When this happens, the reaction system or the model used should be checked for potential problems. For example, in the example presented above, the presence of the supply by transport of the methylperoxy radical (CH_3O_2) in pathways in $P_3 - P_5$ is surprising because CH_3O_2 has a lifetime < 1 minute in the troposphere (Wolfe et al., 2014), and its concentration should be controlled by reactions, not by transport. Similarly, the presence of O transport in pathway D_5 is surprising because O has a small lifetime in the troposphere and the stratosphere. This is the result of an incomplete representation of the chemistry of these species in the reaction system we used. This reaction system comes from a legacy of models designed to study Early Earth and exoplanet anoxic atmospheres. Thus, the reaction system lacks some important reactions for the oxidized modern Earth atmosphere. For this reason, the results presented in section 4.2 should be taken with caution. This example illustrates how Chempath can be a great tool to

understand and validate the results of photochemical models, allowing the modelers to detect potential problems with their reaction systems.

Chempath could also detect well-known and accepted pathways in a photochemical model run. This identification could be an indicator that the model or reaction system used can reproduce results and thus is working as expected. For example, the fact that *Chempath* found the presence of well-known O₃ destruction and production pathways in the *photochem* model suggests that the reaction system we used is partially correct. In particular, the stratospheric chemistry seems to be working as expected. The main purpose of *Chempath* is to understand the results of photochemical models. Whether the pathways detected by *Chempath* are known to be correct or incorrect, these pathways should be interpreted as a product of the analyzed model.

The fact that *Chempath* detected well-known and accepted O₃ production and destruction pathways in our *photochem* model run does not necessarily show that *Chempath* is working correctly. A proper evaluation of *Chempath* would require applying the algorithm in a fully validated model run and doing an inter-comparison with other implementations of the algorithm. For this reason, we encourage the user to use *Chempath* with caution. However, the detection of well-known pathways suggests that our implementation of the pathway analysis program is working as expected and that it can be applied to understand the chemistry of less well-characterized atmospheres, like exoplanet or past atmospheres.

5 Conclusions

In this paper, we described the development of *Chempath*: an open-source pathway analysis program for photochemical models that can automatically construct the most relevant pathways of a reaction system and identify the most important pathways for the production and destruction of a species of interest. We showed how to use *Chempath* in a one-dimensional photochemical model. *Chempath* identified well-known pathways for O₃ destruction and production in Earth's atmosphere, suggesting that this algorithm can be used to understand chemical mechanisms in photochemical models of less well-known atmospheres, like exoplanet or past atmospheres.

Code availability. A frozen version of the code used in this paper is available at <https://doi.org/10.5281/zenodo.13715328>. For up-to-date developments see the *Chempath* GitHub repository: <https://github.com/DanyIvan/chempath>. This repository includes Jupyter notebooks that describe how to run and reproduce the examples presented in this paper.

Author contributions. DGR: Conceptualization, Software, Investigation, Writing - original draft preparation. CG: Supervision, Funding acquisition, Writing - review & editing. ASA: Supervision, Funding acquisition, Writing - review & editing.

Competing interests. We declare that none of the authors has any competing interests.

Acknowledgements. We acknowledge and respect the lək'wəḡən peoples on whose traditional territory the university of Victoria stands and the Songhees, Esquimalt and W̱SÁNEĆ peoples whose historical relationships with the land continue to this day. We thank Ralph Lehmann
485 for answering questions about the pathway analysis program. We thank Aurélien Stolzenbach for pointing to an incorrect reaction in the simple example we used in a previous version of the manuscript. Primary financial support came from Natural Science and Engineering Research Council of Canada (NSERC) Discovery Grants to Colin Goldblatt (RGPIN-2018-05929) and Anne-Sofie Ahm (RGPIN-2022-03912). High-performance computing facilities were provided via a NSERC Research Tools and Infrastructure Grant (RTI-2020-00277).

References

- 490 A. Volz-Thomas, B. R.: Scientific Assessment of ozone depletion:1994, chap. Tropospheric Ozone, World Meteorological Organization,,
<https://csl.noaa.gov/assessments/ozone/1994/>, 1994.
- Androulakis, I. P.: New approaches for representing, analyzing and visualizing complex kinetic transformations, *Computers & Chemical Engineering*, 31, 41–50, <https://doi.org/10.1016/j.compchemeng.2006.05.027>, 2006.
- Arney, G., Domagal-Goldman, S. D., Meadows, V. S., Wolf, E. T., Schwieterman, E., Charnay, B., Claire, M., Hébrard, E., and
495 Trainer, M. G.: The Pale Orange Dot: The Spectrum and Habitability of Hazy Archean Earth, *Astrobiology*, 16, 873–899,
<https://doi.org/10.1089/ast.2015.1422>, 2016.
- Chapman, S.: A Theory of Upper-atmospheric Ozone, *Memoirs of the Royal Meteorological Society*, Edward Stanford, <https://books.google.ca/books?id=Dd0VGwAACAAJ>, 1930.
- Claire, M. W., Kasting, J. F., Domagal-Goldman, S. D., Stüeken, E. E., Buick, R., and Meadows, V. S.: Modeling the signature
500 of sulfur mass-independent fractionation produced in the Archean atmosphere, *Geochimica et Cosmochimica Acta*, 141, 365–380,
<https://doi.org/10.1016/j.gca.2014.06.032>, 2014.
- Clarke, B. L.: Stoichiometric network analysis, *Cell Biophysics*, 12, 237–253, <https://doi.org/10.1007/bf02918360>, 1988.
- Fishtik, I., Callaghan, C. A., and Datta, R.: Wiring Diagrams for Complex Reaction Networks, *Industrial & Engineering Chemistry Research*,
45, 6468–6476, <https://doi.org/10.1021/ie050814u>, 2006.
- 505 Garduno Ruiz, D., Goldblatt, C., and Ahm, A.-S.: Climate shapes the oxygenation of Earth’s atmosphere across the Great Oxidation Event,
Earth and Planetary Science Letters, 607, 118 071, <https://doi.org/10.1016/j.epsl.2023.118071>, 2023.
- Garduno Ruiz, D., Goldblatt, C., and Ahm, A.: Climate Variability Leads to Multiple Oxygenation Episodes Across the Great Oxidation
Event, *Geophysical Research Letters*, 51, <https://doi.org/10.1029/2023gl106694>, 2024.
- Gebauer, S., Grenfell, J., Stock, J., Lehmann, R., Godolt, M., Paris, P. v., and Rauer, H.: Evolution of Earth-like Extrasolar Planetary Atmo-
510 spheres: Assessing the Atmospheres and Biospheres of Early Earth Analog Planets with a Coupled Atmosphere Biogeochemical Model,
Astrobiology, 17, 27–54, <https://doi.org/10.1089/ast.2015.1384>, 2017.
- Grenfell, J. L., Lehmann, R., Mieth, P., Langematz, U., and Steil, B.: Chemical reaction pathways affecting stratospheric and mesospheric
ozone, *Journal of Geophysical Research: Atmospheres*, 111, <https://doi.org/10.1029/2004jd005713>, 2006.
- Haagen-Smit, A. J.: Chemistry and Physiology of Los Angeles Smog, *Industrial & Engineering Chemistry*, 44, 1342–1346,
515 <https://doi.org/10.1021/ie50510a045>, 1952.
- Hu, R., Seager, S., and Bains, W.: Photochemistry In Terrestrial Exoplanet Atmospheres. I. Photochemistry Model And Benchmark Cases,
The Astrophysical Journal, 761, 166, <https://doi.org/10.1088/0004-637x/761/2/166>, 2012.
- Jacob, D. J.: Introduction to Atmospheric Chemistry, Princeton University Press, ISBN 9780691001852, <http://www.jstor.org/stable/j.ctt7t8hg>, 1999.
- 520 Kasting, J. F.: What caused the rise of atmospheric O₂?, *Chemical Geology*, 362, 13–25, <https://doi.org/10.1016/j.chemgeo.2013.05.039>,
2013.
- Kasting, J. F. and Donahue, T. M.: The evolution of atmospheric ozone, *Journal of Geophysical Research: Oceans*, 85, 3255–3263,
<https://doi.org/10.1029/jc085ic06p03255>, 1980.
- Kasting, J. F., Liu, S. C., and Donahue, T. M.: Oxygen levels in the prebiological atmosphere, *Journal of Geophysical Research: Oceans*, 84,
525 3097–3107, <https://doi.org/10.1029/jc084ic06p03097>, 1979.

- Lary, D. J.: Catalytic destruction of stratospheric ozone, *Journal of Geophysical Research: Atmospheres*, 102, 21 515–21 526, <https://doi.org/10.1029/97jd000912>, 1997.
- Lehmann, R.: Determination of Dominant Pathways in Chemical Reaction Systems: An Algorithm and Its Application to Stratospheric Chemistry, *Journal of Atmospheric Chemistry*, 41, 297–314, <https://doi.org/10.1023/a:1014927730854>, 2002.
- 530 Lehmann, R.: An Algorithm for the Determination of All Significant Pathways in Chemical Reaction Systems, *Journal of Atmospheric Chemistry*, 47, 45–78, <https://doi.org/10.1023/b:joch.0000012284.28801.b1>, 2004.
- Milner, P. C.: The Possible Mechanisms of Complex Reactions Involving Consecutive Steps, *Journal of The Electrochemical Society*, 111, 228–232, <https://doi.org/10.1149/1.2426089>, 1964.
- Molina, M. J. and Rowland, F. S.: Stratospheric sink for chlorofluoromethanes: chlorine atom-catalysed destruction of ozone, *Nature*, 249, 810–812, <https://doi.org/10.1038/249810a0>, 1974.
- 535 Schuster, R. and Schuster, S.: Refined algorithm and computer program for calculating all non-negative fluxes admissible in steady states of biochemical reaction systems with or without some flux rates fixed, *Bioinformatics*, 9, 79–85, <https://doi.org/10.1093/bioinformatics/9.1.79>, 1993.
- Segura, A., Kasting, J. F., Meadows, V., Cohen, M., Scalo, J., Crisp, D., Butler, R. A., and Tinetti, G.: Biosignatures from Earth-Like Planets Around M Dwarfs, *Astrobiology*, 5, 706–725, <https://doi.org/10.1089/ast.2005.5.706>, 2005.
- 540 Stock, J., Grenfell, J., Lehmann, R., Patzer, A., and Rauer, H.: Chemical pathway analysis of the lower Martian atmosphere: The CO₂ stability problem, *Planetary and Space Science*, 68, 18–24, <https://doi.org/10.1016/j.pss.2011.03.002>, 2012a.
- Stock, J. W., Boxe, C. S., Lehmann, R., Grenfell, J. L., Patzer, A. B. C., Rauer, H., and Yung, Y. L.: Chemical pathway analysis of the Martian atmosphere: CO₂-formation pathways, *Icarus*, 219, 13–24, <https://doi.org/10.1016/j.icarus.2012.02.010>, 2012b.
- 545 Stock, J. W., Blaszcak-Boxe, C. S., Lehmann, R., Grenfell, J. L., Patzer, A. B. C., Rauer, H., and Yung, Y. L.: A detailed pathway analysis of the chemical reaction system generating the Martian vertical ozone profile, *Icarus*, 291, 192–202, <https://doi.org/10.1016/j.icarus.2016.12.012>, 2017.
- Thompson, M. A., Krissansen-Totton, J., Wogan, N., Telus, M., and Fortney, J. J.: The case and context for atmospheric methane as an exoplanet biosignature, *Proceedings of the National Academy of Sciences*, 119, e2117933 119, <https://doi.org/10.1073/pnas.2117933119>, 2022.
- 550 Tsai, S.-M., Lyons, J. R., Grosheintz, L., Rimmer, P. B., Kitzmann, D., and Heng, K.: VULCAN: An Open-source, Validated Chemical Kinetics Python Code for Exoplanetary Atmospheres, *The Astrophysical Journal Supplement Series*, 228, 20, <https://doi.org/10.3847/1538-4365/228/2/20>, 2017.
- Turányi, T. and Tomlin, A. S.: Sensitivity and Uncertainty Analyses, pp. 61–144, Springer Berlin Heidelberg, ISBN 978-3-662-44562-4, https://doi.org/10.1007/978-3-662-44562-4_5, 2014.
- 555 Verronen, P. T. and Lehmann, R.: Analysis and parameterisation of ionic reactions affecting middle atmospheric HO_x and NO_y during solar proton events, *Annales Geophysicae*, 31, 909–956, <https://doi.org/10.5194/angeo-31-909-2013>, 2013.
- Verronen, P. T., Santee, M. L., Manney, G. L., Lehmann, R., Salmi, S., and Seppälä, A.: Nitric acid enhancements in the mesosphere during the January 2005 and December 2006 solar proton events, *Journal of Geophysical Research: Atmospheres*, 116, <https://doi.org/10.1029/2011jd016075>, 2011.
- 560 Wogan, N.: PhotochemPy: 1-D photochemical model of rocky planet atmospheres, *Astrophysics Source Code Library*, record ascl:2312.011, 2023.

- Wogan, N. F., Catling, D. C., Zahnle, K. J., and Claire, M. W.: Rapid timescale for an oxic transition during the Great Oxidation Event and the instability of low atmospheric O₂, *Proceedings of the National Academy of Sciences*, 119, e2205618119, <https://doi.org/10.1073/pnas.2205618119>, 2022.
- Wogan, N. F., Catling, D. C., Zahnle, K. J., and Lupu, R.: Origin-of-life Molecules in the Atmosphere after Big Impacts on the Early Earth, *The Planetary Science Journal*, 4, 169, <https://doi.org/10.3847/psj/aced83>, 2023.
- Wolfe, G. M., Cantrell, C., Kim, S., III, R. L. M., Karl, T., Harley, P., Turnipseed, A., Zheng, W., Flocke, F., Apel, E. C., Hornbrook, R. S., Hall, S. R., Ullmann, K., Henry, S. B., DiGangi, J. P., Boyle, E. S., Kaser, L., Schnitzhofer, R., Hansel, A., Graus, M., Nakashima, Y., Kajii, Y., Guenther, A., and Keutsch, F. N.: Missing peroxy radical sources within a summertime ponderosa pine forest, *Atmospheric Chemistry and Physics*, 14, 4715–4732, <https://doi.org/10.5194/acp-14-4715-2014>, 2014.
- Zahnle, K., Claire, M., and Catling, D.: The loss of mass-independent fractionation in sulfur due to a Palaeoproterozoic collapse of atmospheric methane, *Geobiology*, 4, 271–283, <https://doi.org/10.1111/j.1472-4669.2006.00085.x>, 2006.